

Title Page.

Quantification of ligand bias for clinically relevant β 2-adrenergic receptor ligands: Implications for drug taxonomy.

Emma T. van der Westhuizen, Billy Breton, Arthur Christopoulos and Michel Bouvier.

Department of Biochemistry and Institute for Research in Immunology and Cancer, University of Montreal,
Montreal, Quebec, Canada (ETvdW, BB and MB). Drug Discovery Biology & Department of Pharmacology,
Monash Institute for Pharmaceutical Sciences, Monash University, Parkville, Victoria, Australia (ETvdW and AC).

Running Title Page.

Running Title: β 2AR ligands are biased toward ERK1/2 signaling.

Corresponding Author: Michel Bouvier

IRIC – Université de Montréal

C.P. 6128 Succursale Centre-Ville

Montreal, Quebec,

Tel: +1-514-343-6319

Fax: +1-514-343- 6843

Email: michel.bouvier@umontreal.ca

Number of text Pages: 42

Number of tables: 4

Number of figures: 8

References: 58

Number of words in abstract: 250

Number of words in introduction: 732

Number of words in discussion: 1487

Non-standard abbreviations:

ALP, alprenolol; ATEN, atenolol; β 2AR, β 2 adrenergic receptor; BET; betaxolol; BIS, bisoprolol; BUC, bucindolol; Ca, calcium; cAMP, cyclic adenosine monophosphate; CARV, carvedilol; Endo, endocytosis ; EPI, epinephrine; ERK1/2, extracellular signal-regulated kinase 1/2; FP: fluorescent protein; FRET fluorescence resonance energy transfer, Gas, stimulatory guanine nucleotide-binding protein; G α i, inhibitory guanine nucleotide-binding protein; GPCR, G protein-coupled receptor; ISO, isoproterenol; LAB, labetalol; MET, metoprolol; NAD, nadolol; NE, norepinephrine; NEB, nebivolol; PIN, pindolol; PRO, propranolol; RET, resonance energy transfer; SALB, salbutamol; SALM salmeterol, TIM, timolol; XAM, xamoterol.

Abstract:

The concepts of functional selectivity and ligand bias are becoming increasingly appreciated in modern drug discovery programs, necessitating more informed approaches to compound classification and, ultimately, therapeutic candidate selection. Using the β 2AR as a model, we present a proof of concept study that assessed the bias of 19 β -adrenergic ligands, including many clinically used compounds, across four pathways (cAMP production, ERK1/2 activation, calcium mobilization and receptor endocytosis) in the same cell background (HEK293S cells). Efficacy-based clustering placed the ligands into five distinct groups with respect to signaling signatures. In some cases, apparent functional selectivity originated from off-target effects on other endogenously expressed adrenergic receptors, highlighting the importance of thoroughly assessing selectivity of the responses before concluding receptor-specific ligand-biased signaling. Eliminating the non-selective compounds did not change the clustering of the 10 remaining compounds. Some ligands exhibited large differences in potency for the different pathways, suggesting that the nature of the receptor-effector complexes influences the relative affinity of the compounds for specific receptor conformations. Calculation of relative effectiveness (within pathway) and bias factors (between pathways) for each of the compounds, using an operational model of agonism, revealed a global signaling signature for all of the compounds, relative to isoproterenol. Most compounds were biased toward ERK1/2 activation over the other pathways, consistent with the notion that many proximal effectors converge on this pathway. Overall, we demonstrate a higher level of ligand texture than previously anticipated, opening perspectives for the establishment of pluridimensional correlations between signaling profiles, drug classification, therapeutic efficacy and safety.

Introduction:

The taxonomy of therapeutic agents has a tremendous impact on preclinical approaches towards discovery and optimization of drug candidates, and on decisions made by clinicians when selecting such agents. Traditionally, most drugs targeting G protein-coupled receptors (GPCRs) have been phenotypically classified as full or partial agonists, (neutral) antagonists or inverse agonists according to their activity at a single canonical signaling pathway. For instance, in the case of the β 2-adrenergic receptor (β 2AR), the many available positive and inverse agonists, as well as neutral antagonists, are generally classified on the basis of their efficacy toward cAMP signaling. However, it is well known that the β 2AR is pleiotropically coupled to many pathways (Evans et al., 2010). Indeed, this is a common observation for most GPCRs and there are increasing instances of ligand behavior changing with the pathway under investigation. For example, some compounds, which are classified as β 2AR neutral antagonists or inverse agonists based on their efficacy toward cAMP, act as agonists toward the ERK1/2 pathway (Azzi et al., 2003; Galandrin and Bouvier, 2006; Shenoy et al., 2006).

The ability of ligands to differentially influence receptor behavior in a pathway-dependent manner has been termed “functional selectivity” or “signaling bias” (Kenakin and Christopoulos, 2013) and can generally be attributed to three sources (Kenakin and Christopoulos, 2013): 1. “system bias”, the relative coupling efficiency of a pathway to the receptor; 2. “observation bias”, the experimental conditions unique to the assay used to measure activity; 3. “agonist or ligand bias”, the ability of a ligand to engender a unique subset of receptor conformations that promotes signaling through distinct pathways to the exclusion of others. It is only the latter form of bias that is associated with the structure of the ligand and receptor and thus reflects a molecular property that can be exploited therapeutically. The phenomenon of ligand bias means that the current taxonomy for β -adrenergic receptor ligands, and probably most GPCR ligands, is likely incorrect, because the classification of any particular ligand can change depending on the pathway under investigation.

Given the increasing discovery of biased ligands in GPCR drug discovery, it is important to develop approaches that can easily quantify the phenomenon in a manner that is experimentally feasible but statistically robust such that it can objectively inform structure-activity studies and compound classification. Significant analytical advances have recently been described that extend the classic operational model of agonism (Black and Leff, 1983) to quantify

ligand bias (Ehlert, 2008; Evans et al., 2011; Figueroa et al., 2009; Kenakin et al., 2012; Kenakin and Christopoulos, 2013; Rajagopal et al., 2011). An important outcome of such analyses is the potential to yield "fingerprints" of compound profiles in a manner that can enrich standard structure-activity and structure-function studies. Ultimately, such detailed fingerprints may be implemented into drug discovery workflows and eventually result in entirely different drug taxonomies that can allow physicians to make better choices in their treatment regime, with fewer adverse effects in the future.

Since the β 2AR is a GPCR with a rich pharmacology and substantial clinical data, it is an ideal candidate for a proof of concept study aimed at developing a chemical biology framework, based on ligand bias determinations, for clustering compounds in a manner that may predict *in vivo* efficacy. As such, we investigated 19 clinically relevant compounds that are used for treating diseases such as asthma, chronic obstructive pulmonary disease, cardiovascular disease, migraine and glaucoma, and determined their signaling efficacy toward four functional outcomes, namely, the cAMP, ERK1/2 and calcium signaling pathways, as well as β 2AR endocytosis. Importantly, both formal clinical studies and anecdotal observations suggest that some of these compounds may be more efficacious and/or safer than others for certain clinical indications, despite having the same relative efficacy toward the cAMP pathway (Eichhorn and Young, 2001; Cruickshank, 1993; Javed and Deedwania, 2009; Ram, 2010; Castle et al., 1993). Although these differences may be attributed to other properties of the drugs (poly-pharmacology, pharmacokinetics, etc.) it is possible that functional selectivity toward different signaling pathways may contribute to their different therapeutic profiles. In depth characterization of the four chosen signaling profiles led to the identification of five sub-groups of ligand with distinct signaling signatures. This represents a first step for establishing more informative links between the *in vitro* cell-based data, whole animal studies and clinical data that may lead to the design of next generation β -adrenergic ligands displaying greater selectivity and reduced side effects profiles.

Materials and Methods:

Adrenergic ligands: (-)-isoproterenol hydrochloride (ISO), (-)-norepinephrine (NE), (-)-epinephrine (EPI), salmeterol xinafoate (SALM), labetalol hydrochloride (LAB), alprenolol hydrochloride (ALP), pindolol (PIN), carvedilol (CARV), bisoprolol hemifumarate (BIS), (\pm)-metoprolol (+)-tartrate salt (MET), timolol maleate salt (TIM), betaxolol hydrochloride (BET), nadolol (NAD), S(-)-atenolol (ATEN), nebivolol hydrochloride (NEB), DL-propranolol hydrochloride (PRO), and CGP-20712A were purchased from Sigma Aldrich (St Louis, MO). ICI 118,551 hydrochloride (ICI), salbutamol hemisulfate (SALB) and xamoterol hemifumarate (XAM) were from Tocris bioscience (Ellisville, MO). Bucindolol (BUC) was a gift from Dr. Michael Bristow (University of Colorado Health Sciences Center, Denver, CO).

Biosensor constructs: GFP₁₀-mutEPAC1(δ DEP; T781A; F782A)-venus (henceforth referred to as EPAC biosensor) was cloned between the NheI and EcoRI sites of pcDNA3.1/zeo(+). The EPAC biosensor consists of an amino-terminal-Green Fluorescent Protein₁₀ (GFP₁₀) joined by a 5 amino acid residue (GSAGT) linker to a mutated EPAC1(δ DEP; T781A; F782A) biosensor (Ponsioen et al., 2004) and a carboxy-terminal-venus fluorescent protein (venus) joined by a 5 amino acid residue linker (KLPAT). This biosensor contains 2 mutations (T781A; F782A), rendering the biosensor inactive with respect to its GEF activity toward Rap1, but maintaining its activation by cAMP (Ponsioen et al., 2004). Deletion of the DEP domain creates a cytosolic EPAC-biosensor, that binds cAMP with micromolar affinity (binding $K_d = 14 \pm 2\mu\text{M}$; Ponsioen et al., 2004). mCherry-obelin was cloned between the NheI and XbaI sites of pcDNA3.1/zeo(+). The obelin biosensor consists of an amino-terminal mCherry joined by 5 amino acid residue linker (GSAGT) to the obelin calcium-activated photoprotein (Illarionov et al., 2000). The obelin biosensor is a bioluminescent photoprotein derived from *Obelia longissima* that tightly binds the chromophore (coelenterazine) with oxygen to form a stable complex, which is activated upon binding 3 calcium ions (linear range of sensitivity: 100nM-100 μM ; Illarionov et al., 2000).

Cell culture and transfections. HEK293S cells stably expressing human $\beta_2\text{AR}$ (Galandrin and Bouvier, 2006) (HEK-HA- $\beta_2\text{AR}$) were confirmed to express 3.17 ± 0.32 pmol/mg protein $\beta_2\text{AR}$ (whole cell binding with [^3H]-CGP12177A). Cells expressing high levels of human $\beta_2\text{AR}$ were selected for this study to enhance the signals

observed for weak partial agonists and inverse agonists. Cells were transiently co-transfected with EPAC biosensor (1500ng/1×10⁶ cells) and mCherry-Obelin (1500ng/1×10⁶ cells) using linear polyethylenimine (1mg/ml) (Polysciences, Warrington, PA) diluted in NaCl (150mM, pH 7.0) (PEI:DNA ratio 3:1) as described (Reed et al., 2006). Cells were used 48h post-transfection for EPAC and obelin measurements.

Phospho-ERK1/2 measurements: Intracellular phospho-ERK1/2 was measured using the Surefire pERK kit (Perkin Elmer, Waltham, MA) using a modified protocol. HEK-HA-β₂AR were plated into 96 well plates (50,000 cells/well) and grown for 32h. Cells were serum starved (DMEM; 0.5% FBS) for 18h prior to ligand stimulation. Increasing concentration of compounds, diluted in DMEM, were added at 37°C for the indicated times to generate full concentration-response curves. Kinetic assays were initially performed using a maximal concentration of ligands, to determine the optimal stimulation time for measuring concentration-response curves (2 or 4 min). Plates were placed on ice, medium aspirated and lysis buffer (proprietary mix included in the kit, 10μl/well) was added. Plates were frozen at -20°C for 18h to ensure complete cell lysis. Lysates were thawed, and a sample from each well (4μl) was transferred to a white 384 well ProxiPlate (Perkin Elmer). Activation buffer (1μl/well), reaction buffer (4μl/well) and AlphaScreen Protein A IgG beads (1:120 dilution) (Perkin Elmer) were mixed, then added to the lysates (5μl/well), in the dark. The lysates were incubated at 25°C for 18h, then the plates were read using the Fusion-αFP with excitation at 680nm (α-laser) and emission at 520-620nm.

EPAC biosensor measurements: HEK-HA-β₂AR were co-transfected with the EPAC and mCherry-obelin biosensors (as described above) then replated into 96 well white CulturePlates (Perkin Elmer) (50,000 cells/well). Cells were serum starved (DMEM, 0.5% FBS) for 18h prior to stimulation. Wells were washed 1x PBS, 1x stimulation buffer (HBSS: 137mM NaCl, 5.4mM KCl, 0.25mM Na₂HPO₄, 0.44 mM KH₂PO₄, 1.8mM CaCl₂, 0.8mM MgSO₄, 4.2mM NaHCO₃, 0.2% (w/v) D-glucose, pH 7.4). Under basal conditions, the GFP₁₀ and venus fluorescent proteins (FPs) are within close proximity, such that upon excitation of the GFP₁₀ with a laser at 400nm, fluorescence resonance energy transfer (FRET) occurs between GFP₁₀ and venus. The light emitted from both FPs is measured using emission filters set at 510nm (GFP₁₀) and 533nm (venus) and FRET ratio (venus emission over GFP₁₀ emission) determined. Upon activation of the EPAC biosensor, a conformational change within the biosensor causes GFP₁₀ and venus to move away from each other, decreasing the FRET between these proteins. Thus,

increases in intracellular cAMP levels are observed as a decrease in the FRET ratio, whereas decreases in the intracellular cAMP levels results in an increase in the FRET ratio. Increasing concentrations of compounds, diluted in HBSS, were added to the wells at 37°C for the indicated times to generate full concentration-response curves. Kinetic assays were initially performed using a maximal concentration of ligands, to determine the optimal stimulation time for measuring concentration response curves (30 min) at 37°C.

Obelin biosensor measurements: HEK-HA- β_2 AR co-transfected with the EPAC biosensor and mCherry-obelin were replated, starved and washed as described for the EPAC measurements above. Cells were pre-incubated with the obelin substrate, coelenterazine cp, (1 μ M; 25°C) for 2h in the dark. Under basal conditions, a low level of calcium-independent luminescence is observed (Illarionov et al., 2000). Upon calcium binding, the photoprotein oxidizes coelenterazine cp, converting it to coelenteramide, releasing carbon dioxide and light in the blue range (465-495nm) (Illarionov et al., 2000). Therefore, with an increase in intracellular calcium levels, an increase in luminescence is observed. Compounds, diluted in stimulation buffer were injected into the wells, and luminescence measured using the SpectraMax L (Molecular Devices, Sunnyvale, CA). Full kinetics were determined for each concentration of ligand (60 sec), and concentration-response curves were determined from the peak calcium responses.

Receptor endocytosis ELISA: HEK-HA- β_2 AR (50,000 cells/well) were plated into white CulturePlates (Perkin Elmer) and grown for 32h, then serum starved (DMEM, 0.5% FBS) for 18h prior to endocytosis assay. Wells were washed 1x PBS, 1x stimulation buffer (HBSS: 137mM NaCl, 5.4mM KCl, 0.25mM Na₂HPO₄, 0.44 mM KH₂PO₄, 1.8mM CaCl₂, 0.8mM MgSO₄, 4.2mM NaHCO₃, 0.2% (w/v) D-glucose, 0.5% (w/v) bovine serum albumin, pH 7.4) (SB). Increasing concentration of compounds, diluted in HBSS, were added at 37°C for the indicated times to generate full concentration-response curves. Kinetic assays were initially performed using a maximal concentration of ligands, to determine the optimal stimulation time for measuring concentration-response curves (30 min). Plates were placed on ice, stimulation buffer aspirated and cells fixed with paraformaldehyde (3% w/v) for 10 min at 23°C. Cells were washed (3x 10 min, SB) before the addition of anti-HA-HRP (3F10; 1:3000) (Roche, IN, USA) (18h, 4°C). Following, cells were washed (3x 10 min, SB), Vybrant dye (Invitrogen, 1:2000) was added (30 min, 25°C) and cells were washed again (3x 10 min, SB). Vybrant fluorescence was measured with excitation at 480nm and

emission at 538nm auto cutoff 530nm using the FlexStationII (Molecular Devices), to control for the number of cells/well. Western lightning-plus ECL (Perkin Elmer) was added to the wells (50µl/well) and incubated for 1 min in the dark, then chemiluminescence was measured for 1 sec/well in the SpectraMaxL (Molecular Devices)

Preparation of ligands: All ligands were prepared from powder immediately prior to each experiment, in vehicle and used immediately. All compounds were diluted from stock solutions (10mM) into stimulation buffer (HBSS (cAMP, calcium and ELISA assays) or DMEM (ERK1/2 assays). Since ISO is susceptible to oxidation, ascorbate is often used to prevent oxidation. However, we elected not to systematically use ascorbate in our experiments, because we found that low concentrations of ascorbate (34nM) directly activate ERK1/2 signaling in HEK-HA-β2AR cells in a rapid and transient manner (Supplemental Figure 1). This would have a significant impact on the quantification of signaling biases of the adrenergic ligands at the β2AR. To confirm that the oxidation of ISO in the experiments had no significant effect on the cAMP assay (the assay with the longest duration; 30 min), the kinetics and concentration-response curves to ISO were compared in stimulation buffer with or without ascorbate (0.1mM) (Supplemental Figure 2). Since no significant effect was observed on the ISO-stimulated cAMP responses with or without ascorbate, we concluded that there would be no impact on the bias calculations if ascorbate was excluded from the stimulation buffer.

Data Analysis: For each assay, data were normalized as percentage of the maximal isoproterenol-stimulated response. All values are expressed as mean ± standard error of the mean of n experiments. The operational model (Black and Leff, 1983) was used to determine the transduction ratios (τ/K_A) of the agonists using equation 5, derived from the standard form of the operational model by equations 1:

$$E = Basal + \frac{(E_m - Basal)\tau^n [A]^n}{\tau^n [A]^n + ([A] + K_A)^n} \quad \text{EQN 1}$$

Where the ‘Basal’ parameter was added for fitting non-zero basal responses. Dividing through by K_A yields the τ/K_A ratio by equation 2:

$$E = Basal + \frac{(E_m - Basal) \left(\frac{\tau}{K_A} \right)^n [A]^n}{\left(\frac{\tau}{K_A} \right)^n [A]^n + \left(\frac{[A]}{K_A} + 1 \right)^n} \quad \text{EQN 2}$$

The τ/K_A was redefined as the single fitted parameter, R such that:

$$E = Basal + \frac{(E_m - Basal) R^n [A]^n}{R^n [A]^n + \left(\frac{[A]}{K_A} + 1 \right)^n} \quad \text{EQN 3}$$

The equation was then simplified by dividing above and below by $R^n [A]^n$ by:

$$E = Basal + \frac{(E_m - Basal)}{1 + \left(\frac{\left(\frac{[A]}{K_A} + 1 \right)}{R \times [A]} \right)^n} \quad \text{EQN 4}$$

For curve-fitting purposes, the parameters, K_A and R were re-cast as logarithms (i.e., $10^{\text{Log}K_A}$, $10^{\text{Log}R}$), yielding the final equation used for direct curve-fitting:

$$E = Basal + \frac{(E_m - Basal)}{1 + \left(\frac{\left(\frac{[A]}{10^{\text{Log}K_A} + 1 \right)}{10^{\text{Log}R} \times [A]} \right)^n} \quad \text{EQN 5}$$

where E is the effect of the ligand, [A] is the concentration of agonist, E_m is the maximal possible response of the system, Basal is the basal level of response in the absence of agonist, $\text{Log}K_A$ denotes the logarithm of the functional equilibrium dissociation constant of the agonist, n is the slope of the transducer function that links occupancy to response, and $\text{Log}R$ is the logarithm of the “transduction coefficient” (or “transduction ratio”), τ/K_A , where τ is an index of the coupling efficiency (or efficacy) of the agonist. For more details, see Evans et al. (2011), Kenakin et al., (2012) and Kenakin and Christopoulos (2013). For the analysis, all families of agonist curves at each pathway were globally fitted to the model with the parameters, Basal, E_m and n shared between all agonists. For full agonists, the $\text{Log}K_A$ was constrained to a value of zero¹, whereas for partial agonists this was directly estimated by the curve fitting procedure. The $\text{Log}R$ (i.e., $\log(\tau/K_A)$) parameter was estimated as a unique measure of activity for each agonist.

The relationship between the Black-Leff model and the parameters that describe the standard empirical logistic equation (i.e., EC_{50} and E_{max}) has been described previously (Black et al., 1985; Kenakin et al., 2012). In brief,

$$[EC_{50}] = \frac{K_A}{(2+\tau^n)^{1/n}-1} \quad \text{EQN 6}$$

and

$$E_{max} = \frac{E_m \tau^n}{1+\tau^n} \quad \text{EQN 7}$$

All data were analyzed using the non-linear curve fitting equations in Graphpad Prism (v6.0) to estimate the pEC₅₀ values of the curves for the different pathways. Ligand bias was quantified by analyzing the concentration-response curves using the operational model of agonism, as described previously (Evans et al., 2010; Kenakin et al., 2012) according to equation 5 (see appendix 1 for GraphPad Prism equations and fitting parameters).

The assessment of true ligand bias requires the elimination of the influence of system and observation bias to the observed functional selectivity (Kenakin and Christopoulos, 2013). This is achieved by comparing ligand activity at a given signaling pathway to that of a reference compound. In our study, ISO was selected as the reference compound because it did not activate any of the four pathways through other adrenergic receptors, and had similar potencies toward all four signaling pathways. Thus, to determine the relative effectiveness of the compounds to activate the different signaling pathways, the difference between the log(τ/K_A) values was calculated using equation 8:

$$\Delta \log \left(\frac{\tau}{K_A} \right) = \log \left(\frac{\tau}{K_A} \right)_{LIGAND} - \log \left(\frac{\tau}{K_A} \right)_{ISO} \quad \text{EQN 8}$$

The compounds' effectiveness toward each pathway, relative to ISO, were calculated as the inverse logarithm of the $\Delta \log(\tau/K_A)$ using equation 9:

$$relative\ effectiveness = 10^{\Delta \log \left(\frac{\tau}{K_A} \right)} \quad \text{EQN 9}$$

Ligand bias was calculated using equations 10 and 11, as the difference between the $\Delta \log(\tau/K_A)$ values derived from equation 8:

$$\Delta \Delta \log \left(\frac{\tau}{K_A} \right) = \Delta \log \left(\frac{\tau}{K_A} \right)_{L1:P1} - \Delta \log \left(\frac{\tau}{K_A} \right)_{L2:P2} \quad \text{EQN 10}$$

$$bias\ factor = 10^{\Delta \Delta \log \left(\frac{\tau}{K_A} \right)} \quad \text{EQN 11}$$

where L1 is ligand 1, P1 is pathway 1 and P2 is pathway 2.

The standard error of the mean was calculated for the transduction ratios $\log(\tau/K_A)$ using equation 12

$$SEM = \frac{\sigma}{\sqrt{n}} \quad \text{EQN 12}$$

where σ is the standard deviation and n is the number of experiments. To avoid propagation of the error through the multiple subtraction steps, the estimated standard errors for each ligand and each pathway were calculated using equations 13 and 14.

$$SE\left(\log\left(\frac{\tau}{K_A}\right)\right) = \sqrt{(SEM_{L1})^2 - (SEM_{L2})^2} \quad \text{EQN 13}$$

$$SE\left(\Delta\log\left(\frac{\tau}{K_A}\right)\right) = \sqrt{\left(SE\left(\log\left(\frac{\tau}{K_A}\right)\right)_{L1:P1}\right)^2 - \left(SE\left(\log\left(\frac{\tau}{K_A}\right)\right)_{L2:P2}\right)^2} \quad \text{EQN 14}$$

where L1 is ligand 1, L2 is ligand 2, P1 is pathway 1 and P2 is pathway 2. A detailed set of instructions on how to calculate biases with examples taken from this study are included as appendix 1.

Statistical analysis was performed using a two-way unpaired student's t-test on the $\Delta\log(\tau/K_A)$ ratios to make pairwise comparisons between two pathways activated by a given ligand, where $p < 0.05$ was considered to be statistically significant.

Results:

Different potency and efficacy profiles were observed for adrenergic ligands toward 4 distinct signaling outputs:

Initially, 17 β -adrenergic ligands currently used in various clinical indications (Javed and Deedwania, 2009; Ram, 2010; Cruickshank, 1993; Eichhorn and Young, 2001; Castle et al., 1993) and 2 endogenous ligands were selected to assess their functional selectivity towards 4 signaling pathways: cAMP production, calcium mobilization, ERK1/2 activation and receptor endocytosis (Tables 1 and 2). For reference purposes, the compounds, structures, binding affinities (from published radio-ligand binding studies), relative efficacies (previously reported for cAMP production), receptor subtype selectivity profile and clinical uses are provided for each compound (Table 1). The first step to quantify the ligand biases at the β 2AR was to carefully select the test ligands and determine full concentration-response curves for the different pathways for all ligands. Second, signaling efficacy was analyzed using the operational model curve fitting parameters and finally ligand biases were calculated (see Methods and Appendix 1). The maximal response (E_{\max}) and the potency (pEC_{50}) for each compound demonstrate that each has a unique signaling signature (Table 2).

Some adrenergic ligands activate signaling pathways through multiple adrenoceptor subtypes:

Several compounds included in this study were reported to act at other adrenergic receptor subtypes (Table 1). To eliminate possible confounding effects resulting from activation of other endogenously expressed adrenergic receptors, a single concentration of each agonist (pEC_{50} - pEC_{80} toward a particular signaling output) was tested in cells pre-treated (60 min) with adrenergic antagonists at concentrations that fully occupy the targeted receptors with marginal occupancy (less than 11% of β 2AR occupancy for all ligands) of the other receptor subtypes (β 1AR: CGP-20712A (100nM, 11% occupancy at β 2AR), β 2AR: ICI 118,551 (100nM, 100% occupancy at β 2AR), α 1AR: prazosin (10nM, >0.01% occupancy at β 2AR), α 2AR: rauwolscine (100nM, 0.2% occupancy at β 2AR)) (Figure 1). These compounds were selected for their lack of intrinsic efficacies on the pathways tested except for ICI 118,551, which was an inverse agonist towards cAMP (Supplemental Figure 3 and Table 2).

The responses for seven of the compounds (EPI, NE, ALP, PRO, ATEN, TIM, BET) were partially inhibited by a non- β 2AR antagonist, suggesting that some of their activity originates from binding to a different adrenergic receptor subtype (Figure 1). While activation of the cAMP, calcium and endocytotic pathways by the agonist compounds were all β 2AR specific, (defined by sensitivity to antagonism by ICI 118,151 but not CGP-20712A, prazosin, or rauwolscine), the ERK1/2 activation promoted by some of the compounds (EPI, NE, ALP and PRO) involved the α 2AR (NE and EPI), α 1AR (PRO) or both (ALP). To determine whether the endogenously expressed α 1AR and α 2AR could activate ERK1/2 signaling in the HEK-HA- β 2AR cells, the effects of the α 1AR agonist, phenylephrine (PE) and the α 2AR agonist, UK14304 (brimonidine) were tested (Supplemental Figure 4). ERK1/2 was activated by PE and UK14304 in the HEK-HA- β 2AR cells, demonstrating that the endogenously expressed α 1AR and α 2AR were coupled to ERK1/2 signaling and could contribute to the overall ERK1/2 responses observed in the HEK-HA- β 2AR cells. Although activation of multiple receptors contributes to the signaling textures of these ligands, the contribution of additional receptors to the response profile greatly complicates the interpretation of potential ligand-biased signaling through the β 2AR (system bias). These ligands were excluded from further experiments and analysis in order to eliminate the “system bias” from the calculations of the true “ligand bias” at the β 2AR. Several compounds (ATEN, TIM, NEB and MET) yielded weak (low efficacy or potency) inhibition of cAMP production, resulting in variability of the signal that made it difficult to clearly establish whether the responses were β 2AR-specific. These inverse agonists, as well as BET (antagonized by prazosin), were also excluded from further analysis (Figure 1). Taken together, these data emphasize the importance of assessing the pharmacological target-based selectivity of the response studied before concluding that the different response profiles result from ligand biased signaling through a common receptor.

To further assess the β 2AR-selectivity of the remaining compounds, the ability of the β 2AR selective ligand ICI 118,551 to inhibit the concentration-dependent responses evoked by ISO, SALB, SALM, LAB, BUC, PIN, XAM, CARV, BIS and NAD was tested. As shown in Figure 2, pre-treatment with 10nM or 1 μ M ICI 118,551 right-shifted the cAMP concentration response curves to ISO, SALB, SALM, LAB, BUC and PIN in a manner characteristic of classical competitive antagonism. Similarly, the ERK1/2 responses promoted by ISO, SALB, SALM, LAB, BUC, PIN, XAM and CARV (Figure 3), the calcium mobilization induced by ISO, SALB and SALM (Figure 4) and the

endocytosis stimulated by ISO and SALB (Figure 5) were also antagonized by ICI 118,551. However, in some cases, the inhibition appeared non-competitive most likely due to the fact that ICI 118,551 did not fully dissociate from the receptor within the time frame of the functional assay (1-2 min). In any case, the ability of ICI 118,551 to right shift the concentration-response curves confirmed that these responses were mediated by the β 2AR. Similarly, the fact that no further inhibition of the cAMP production could be promoted by BIS and NAD following the pre-treatment with ICI 118,551 confirmed that these inverse agonist activities were β 2AR specific and that ICI 118,551 is an inverse agonist at the β 2AR for the cAMP response (Figure 6).

Based on their efficacy profiles (Table 2), the 10 compounds with β 2AR-selective responses fall into 5 different clusters: 1. agonists for 4 pathways (ISO and SALB); 2. agonists for 3 pathways (SALM); 3. agonists for 2 pathways (LAB, BUC and PIN); 4. agonists for 1 pathway (XAM and CARV); 5. inverse agonists on 1 pathway (BIS and NAD). Each of these clusters is described in more detail below.

Multifarious ligands activating four pathways (cAMP, ERK1/2, calcium and receptor endocytosis):

Although four compounds activated all four pathways, β 2AR-selectivity was only observed for two compounds, ISO and SALB (Figure 7A-B). To compare the relative efficacies of the compounds, ISO was used as the reference compound and all data were expressed as a percentage of the maximal stimulation promoted by ISO. Considering the potencies toward the different pathways, ISO showed no significant selectivity, with similar pEC₅₀ values for the 4 signaling modalities (Table 2; Figure 7A). In contrast, SALB had different potencies toward the different pathways; the rank order of potency being ERK>cAMP>calcium>endocytosis with a spread of more than 4 logarithmic units difference between the most and least responsive signaling modalities (Table 2 and Figure 7B). The maximum agonist effects of SALB toward cAMP production and ERK1/2 activation were similar to ISO. However, SALB behaved as a partial agonist toward both calcium mobilization and endocytosis, resulting in 50% and 45% of the maximal ISO responses for these two pathways, respectively. These data demonstrate that SALB is a functionally selective ligand and also suggest that the 4 pathways downstream of the β 2AR are, at least in part, independent from each other.

A ligand deficient in β 2AR endocytosis:

SALM was the only compound that activated cAMP, ERK1/2 and calcium without promoting β 2AR endocytosis (Table 2 and Figure 7C). For the 3 other pathways, the order of potency for SALM was the same as that observed for SALB (ERK>cAMP>calcium). SALM was a full agonist toward ERK1/2 and cAMP but a partial agonist toward calcium (34% of the maximal isoproterenol-stimulated response), similar to what was observed for SALB.

Ligands that activated two pathways (cAMP and ERK1/2):

LAB, BUC and PIN all activated cAMP production and ERK1/2 but not calcium mobilization or β 2AR endocytosis (Table 2; Figure 7D-F). LAB was significantly more potent toward the ERK1/2 than the cAMP pathway, with differences of 2 logarithmic units between the two pathways. LAB was a full agonist for the ERK1/2 pathway (107% of the ISO-stimulated response), but was a partial agonist for cAMP production (52% of the ISO-stimulated response) (Table 2; Figure 7D). In contrast to LAB, PIN and BUC had similar potencies toward the two pathways. PIN was a partial agonist toward the cAMP and ERK1/2 pathways (18% and 62% of the ISO-stimulated response, respectively) whereas BUC was a partial agonist toward cAMP but a full agonist toward ERK1/2 (62% and 107% of the ISO-stimulated response, respectively) (Table 2; Figure 7E-F). In addition, BUC and PIN promoted bell-shaped ERK1/2 responses, indicating that at higher concentrations they inhibit this pathway, thus further distinguishing them from the other ligands.

Agonists or inverse agonists that activated (ERK1/2) or inhibited (cAMP) only one pathway:

XAM and CARV were neutral ligands toward all pathways, except for selectively activating ERK1/2 through the β 2AR, indicating a very high level of functional selectivity (Figure 7G-H). XAM activated the ERK1/2 pathway to a similar extent as ISO (103% of the ISO-stimulated response) whereas CARV acted as a partial agonist (85% of the ISO-stimulated response). CARV promoted a biphasic activation profile similar to those observed for BUC and PIN, in contrast to XAM that activated ERK1/2 in a monophasic manner. The activation of the ERK1/2 signaling pathway, in the absence of any of the other signaling modalities, suggests that β 2AR-promoted ERK1/2 activation was independent from cAMP production, calcium mobilization or receptor endocytosis. In contrast to the lack of significant CARV-stimulated endocytosis that we observed ($6.7 \pm 12.0\%$), CARV was previously shown to induce a small yet statistically significant β 2AR internalization ($5.5 \pm 1.7\%$) in HEK293 cells (Wisler et al., 2007). Yet, as in

the present study, the CARV-induced endocytosis was found to be marginal when compared to the ISO-stimulated internalization ($38.7 \pm 3.5\%$ in Wisler et. al., 2007 and $53.6 \pm 2.7\%$ in our study). Thus the difference between the two studies is quantitative and not qualitative and probably due to a different sensitivity of the assays used to measured endocytosis.

Although six compounds were inverse agonists for the cAMP pathway, only two compounds (BIS and NAD) were selectively acting at the $\beta 2AR$ (Figure 1). When compared to the maximal stimulatory activity of ISO, NAD and BIS promoted inhibitory responses of -34% and -13%, respectively (Figure 7I-J).

Quantification of ligand bias:

As shown in table 2, the potencies and efficacies toward the different pathways varied significantly among the compounds, suggesting the occurrence of biased signaling. In order to quantify this bias, we applied the operational model to derive transduction ratios (τ/K_A) as a distillation of the effect of the compounds on receptor conformations underlying the different signaling modalities. The transduction ratios and resulting bias factors are shown in tables 3 and 4. Since ISO displayed similar potencies and hence, similar (τ/K_A) ratios between pathways, this was utilized as the reference agonist against which all *within-pathway* comparisons to the other agonists were made ($\Delta \log(\tau/K_A)$). The responses to ISO for all four pathways yielded similar potencies, revealing ISO as functionally distinct from the other test compounds. Since the potencies for ISO towards all pathways were similar, the variable potencies observed for the other ligands could not be attributed to differences in the level of amplification between the signaling pathways nor the assay sensitivity. These features of ISO made it an ideal candidate for a reference compound at the $\beta 2AR$, and a better choice than EPI, the endogenous ligand for the $\beta 2AR$, since EPI activated ERK1/2 via endogenously expressed αARs in addition to the overexpressed $\beta 2ARs$ (Figure 1). As previously highlighted (Kenakin and Christopoulos, 2013), ligand bias is a relative term; without comparison to a reference agonist to cancel out the influence of system and observation biases, true ligand bias cannot be determined. Subsequently, *between-pathway* comparisons were made for a given ligand in the form of the final bias factor ($\Delta \Delta \log(\tau/K_A)$). Since ISO oxidizes, it was important to verify that any signaling bias calculated in reference to this compound did not result from a change in the actual concentration during the course of the experiment. For this purpose, time- and dose-dependent ISO-promoted cAMP production was monitored by the EPAC biosensor in the

presence and absence ascorbate. As shown in Supplemental Figure 2, the addition of ascorbate did not significantly affect either the kinetics or the dose response curves obtained. Since cAMP was the assay involving the longest time of incubation, the oxidation of isoproterenol did not influence the ligand biases calculated in the present study. This suggests that in the time frame of the experiments (30 min) and at the temperature used (37°C), only marginal oxidation occurs.

Comparison of the bias factors for each ligand between the different pathways revealed that, relative to ISO, many ligands were biased for the ERK1/2 pathway over the cAMP pathway, the cAMP pathway over calcium mobilization, whereas there was no bias for calcium over β 2AR endocytosis (Figure 8 and Table 4). Together, this suggests that there was a rank order of pathway bias for all of the compounds tested at the β 2AR (ERK>cAMP>calcium=endocytosis). LAB was the compound with the strongest bias toward the ERK1/2 over cAMP, activating ERK1/2 signaling 1108-fold better than cAMP signaling. SALB and SALM for their part were 62- and 19-fold better at activating ERK1/2 than cAMP, respectively (Table 4). The biases of SALB and SALM toward cAMP over calcium were 3- and 17-fold, respectively, whereas they were 183- and 316-fold for ERK over calcium (Table 4). SALB was 4-fold better at activating cAMP over endocytosis and 223-fold better at activating ERK1/2 than endocytosis. PIN and BUC that could activate only cAMP and ERK1/2 signaling were not significantly biased for either of the two pathways (Table 4). Bias factors were not calculated for all pathways for all ligands since the absence of stimulation of a pathway prevents the calculation of a τ/K_A ratio. However, when a pathway was not activated by a ligand, it may be indicative that the bias was even greater than the largest bias that could be calculated between the two pathways considered. For example, CARV and XAM, which could activate ERK1/2 but not cAMP, calcium or receptor endocytosis (Table 2, Figure 3), may be activating ERK1/2 at least 1108-fold better than cAMP, 316-fold better than calcium and 223-fold better than endocytosis. Alternatively, if the lack of effect is solely due to weak coupling efficiency, then any underlying bias may not be as extreme.

Because the system used to test the bias would be predicted to influence the biases observed toward different pathways, as a result of the different relative concentration of the signaling partners and their responsiveness, we tested the cAMP and ERK1/2 responses in a different system for three compounds that showed a strong bias toward ERK1/2 vs. cAMP in the HEK-HA- β 2AR cells. For this purpose we used the parental HEK293S cells that express a

very low level of β 2AR. As can be seen in Supplemental Figure 5 and Supplemental Table 1, LAB could not evoke any detectable cAMP or ERK1/2 response in cells expressing such a low level of receptor. Both SALM and SALB did stimulate the two pathways, however, in contrast to what was observed in the over-expressing HEK-HA- β 2AR, SALB was not biased toward either the ERK1/2 or cAMP pathways, whereas SALM was slightly biased toward ERK with an ERK-cAMP bias factor of 1.74 (Supplemental Tables 2 and 3). These results dramatically demonstrate the importance of the system in the observed bias.

Discussion:

Functional selectivity is likely to be a widespread phenomenon underlying drug action at GPCRs. At the molecular level, this reflects ligand bias ('biased agonism'), the ability of different ligands to stabilize distinct conformational ensembles of receptor-transducer pairs at the expense of others, the consequence being signal pathway-selectivity. Although relative bias is clearly a property of a given ligand-receptor couple it is also influenced by the system in which it is measured. To exploit ligand bias in a manner that can assist structure-activity studies or compound classification/selection strategies, it is necessary to utilize methods that remove observational biases on functional selectivity, as well as ensuring that the cell-based behavior truly reflects on-target, rather than off-target effects. Our study highlights both of these phenomena as well as the influence of the system on the observed biases.

The systematic analysis outlined in this study, using nineteen β -adrenergic ligands and four distinct pathways (cAMP, ERK1/2 calcium and receptor endocytosis), revealed that despite overexpression of the target β 2AR, many ligands have detectable efficacy towards other endogenously expressed adrenoceptors in HEK293S cells. Due to the confounding effects that the stimulation of more than one receptor subtype has on the signaling outcomes, biases cannot be determined for such ligands. Yet, this is useful information as these off-target effects may contribute to either the therapeutic efficacy or undesirable effects of drugs.

For ligands acting selectively through the β 2AR, the operational model revealed a rank order of pathway bias (ERK>cAMP>Ca=endocytosis) for three of the agonists tested (SALB, SALM, LAB,) relative to ISO. Compounds with neutral or inverse efficacies cannot be included in the formal bias analysis yet they are clearly favoring different receptor conformations than the agonists. The different signaling profiles, based on the ability of the compounds to activate specific pathways, clustered into five groups, potentially representing the propensity of each of these ligand groups to stabilize different receptor-effector complexes. Given that some compounds evoked biphasic concentration-response curves, one could also include this as a criteria to cluster the ligands into seven groups rather than five, to account for the unusual behavior of these ligands. Collectively, this study presents a framework for the quantitative evaluation of GPCR ligand bias in a manner that can facilitate more informed compound classification and, if implemented as a routine approach in drug discovery workflows, preclinical drug candidate selection.

One striking observation was that all compounds, except for BUC and PIN, were significantly biased for ERK1/2 signaling over the other pathways relative to ISO. In addition, when a single pathway was activated by a ligand (e.g. CARV and XAM), it was always ERK1/2. The mechanism underlying such prevalence of the ERK1/2 pathway is unknown but could be explained by the fact that many effectors (*Gas*, *G α i*, β -arrestin) couple the β 2AR to the ERK1/2 pathway (Azzi et al., 2003; Daaka et al., 1997; Keiper et al., 2004). Consistent with this notion, several of the compounds (BUC, PIN and CARV) activated ERK1/2 in a biphasic manner, a phenomenon that can result from ligand-promoted activation of several concurrent signaling pathways (Rovati and Nicosia, 1994; Dittman et al., 1994). Of note, many ligands that activated ERK1/2 did so in the absence of any detectable endocytosis. Given the proposed role of β -arrestin (Azzi et al., 2003; Shenoy et al., 2006) and β -arrestin-mediated endocytosis (Daaka et al., 1998) in the ISO-stimulated ERK1/2 activity, it will be of interest to determine the signaling pathways underlying the activation by ligands that do not promote endocytosis.

For all compounds tested, calcium was a less preferred pathway being either weakly or not stimulated, even for compounds that maximally stimulated ERK1/2 or cAMP, indicating that this pathway is at least in part independent from the cAMP and ERK responses. The exact mechanism responsible for the calcium mobilization in the HEK-HA- β 2AR cells used in the present study is unknown, but could occur via a *Gs*-cAMP-EPAC-Rap2B-PLC ϵ -dependent pathway, as in HEK293 cells (Schmidt et al., 2001), a *Gs*-cAMP-PKA-dependent pathway, as in cardiomyocytes or rat hippocampal neurons (Zhang et al., 2001; Tzingounis et al., 2010) or via *Gi*, as in cardiomyocytes (Zhang et al., 2001). Alternatively, it could be due to a crosstalk between the *Gs*-coupled β 2AR and *Gq*-promoted IP3 productions as in mouse airway smooth muscle cells overexpressing the β 2AR (McGraw et al., 2003). Determining which pathway is responsible for the calcium responses observed in the present study as well as the molecular basis for the bias observed opens interesting new avenues.

The importance of the system used to assess ligand biases was clearly illustrated by the difference in the bias values obtained in two cell lines expressing different β 2AR levels. Consistent with the notion that the effectiveness toward a given pathway is defined by the ligand's affinity (K_A) and the stimulus-effect (E/S) relationship (Black and Leff, 1983) for this pathway, our data show different transduction ratios ($\text{Log}(\tau/K_A)$) for the two cell systems; the ERK1/2

pathway being more affected than cAMP. These changes were not equivalent for all ligands, consistent with the notion of bias. The specific mechanisms responsible for these system-dependent differences are not known but could be linked to the relative expression levels of the receptor vs. effectors, the constitutive activity or the desensitization state of the different components involved.

The prevailing hypothesis to explain functional selectivity proposes that different ligands promote or stabilize different receptor conformation(s) with preferential affinities for subsets of effectors. Recent structural studies on the β 2AR confirmed that different compounds stabilized distinct receptor conformations (Rasmussen et al., 2007; Wacker et al., 2010), consistent with this notion. However, the recent findings that the effectors contributed to the conformational changes undergone by a receptor and that these conformational changes were translated into altered affinities for the ligands (Rasmussen et al., 2011) suggest that assembly of receptor-effector complexes before ligand binding could contribute to functional selectivity. This hypothesis is supported by our study, where the distributions of potencies of a given compound for activation of distinct signaling pathways were observed to be as vast as four orders of magnitude (e.g. SALB potency for ERK1/2 vs. endocytosis).

The influence that effector can have on receptor conformation and hence ligand affinity is taken into account by the approach used in the present study where the τ/K_A ratios used to assess biases are derived directly from the concentration-response curves that take into account differences in ligand affinities for the different agonist-receptor-effector complexes (Kenakin et al., 2012). This is different from other approaches using affinity (pKd) values derived from competition binding experiments against a single radioligand to calculate τ values. Indeed, such approaches assume that the affinity of the ligand for the receptor-effector complex is the same in the activation of all signaling pathways. Given that different affinity values can be obtained for a given compound when determined in competition against different radioligands (e.g. ISO pKd obtained when using different radioligands: [125 I]-pindolol = 7.54 (Del Carmine et al., 2002); [3 H]-CGP12177A = 6.64 (Baker, 2010); [3 H]-epinephrine = 8.68 (U'Prichard et al., 1978)), the affinity of compounds toward a particular agonist-receptor-effector complex using a single binding affinity value may introduce a probe-dependency into the calculation of signaling bias. Using this approach SALM was biased for β -arrestin recruitment over cAMP signaling (Rajagopal et al., 2011), which is surprising given that SALM did not promote β 2AR endocytosis measured by cell-surface ELISA (Table 2; Drake et al., 2008) or confocal

microscopy (Moore et al., 2007). This apparent paradox could result from the method used to calculate biases as suggested above. Alternatively, it could be explained if SALM stabilizes a β 2AR- β -arrestin complex unable to endocytose. Consistent with this possibility, differences in biased agonism for β -arrestin recruitment vs. β -arrestin rearrangements were recently reported (Zimmerman et al., 2012). The differences could also be explained by the use of a chimeric β 2AR-vasopressin 2 receptor in the Rajagopal (2011) study for the β -arrestin recruitment assays.

Calculating bias factors for ligands and signaling pathways adds a new level of texture in examining drug responses. Examples of compounds with differences in their therapeutic activity, possibly resulting from functional selectivity, are starting to emerge (Violin et al., 2013). The present study has broadened the notion of ligand bias and expanded the information available regarding the efficacy of β -adrenergic ligands at the β 2AR. In addition it provided a framework to systematically compare a large number of ligands for diverse signaling pathways. Further studies will be needed to establish the links between the signaling signatures, the therapeutic efficacy, the safety profiles and the chemical structures of the compounds in specific signaling clusters in physiologically relevant cell lines and whole animal models. This is still a significant challenge especially when considering the importance of the system used (e.g.: cell types, receptor and effector expression levels, etc...) to determine the signaling biases. However, applying a systematic approach such as the one describe herein across different systems should allow the classification of compounds into functionally distinct clusters that should facilitate the design of drugs with increased therapeutic efficacy and reduced side effect profiles.

Acknowledgements:

The authors would like to thank Dr. Monique Lagacé for critical reading of the manuscript and assistance with preparation of the figures and Wayne Stallaert for discussion on different aspects of experimental design and data analysis. We would also like to thank Christian Charbonneau for assistance in the preparation of figure 8.

Authorship contributions:

Participated in research design: van der Westhuizen and Bouvier.

Conducted experiments: van der Westhuizen

Contributed new reagents or analytical tools: Breton, Christopoulos

Performed data analysis: van der Westhuizen

Wrote or contributed to the writing of the manuscript: van der Westhuizen, Christopoulos and Bouvier

References:

Azzi M, Charest PG, Angers S, Rousseau G, Kohout T, Bouvier M, and Pineyro G (2003). Beta-arrestin-mediated activation of MAPK by inverse agonists reveals distinct active conformations for G protein-coupled receptors. *Proc Nat Acad Sci USA* **100**(20): 11406-11411.

Baker JG (2010). The selectivity of beta-adrenoceptor agonists at human beta1-, beta2- and beta3-adrenoceptors. *Br J Pharmacol* **160**(5): 1048-1061.

Baker JG (2005). The selectivity of beta-adrenoceptor antagonists at the human beta1, beta2 and beta3 adrenoceptors. *Br J Pharmacol* **144**(3): 317-322.

Baker JG, Hall IP, and Hill SJ (2003). Agonist and inverse agonist actions of beta-blockers at the human beta 2-adrenoceptor provide evidence for agonist-directed signaling. *Mol Pharmacol* **64**(6): 1357-1369.

Baker JG, Hill SJ, and Summers RJ (2011). Evolution of β -blockers: from anti-anginal drugs to ligand-directed signalling. *Trends Pharmacol Sci* **32**(4):227-34.

Black JW and Leff P (1983). Operational models of pharmacological agonism. *Proc R Soc Lond B Biol Sci* **220**(1219): 141-162.

Black JW, Leff P, Shankley NP and Wood J (1985). An operational model of pharmacological agonism: the effect of E/[A] curve shape on agonist dissociation constant estimation. *Br J Pharmacol* **84**(2): 561-571.

Castle W, Fuller R, Hall J, and Palmer J (1993). Serevent nationwide surveillance study: comparison of salmeterol with salbutamol in asthmatic patients who require regular bronchodilator treatment. *Brit Med J* **306**(6884): 1034-1037.

Chidiac P, Hebert TE, Valiquette M, Dennis M, and Bouvier M (1994). Inverse agonist activity of beta-adrenergic

antagonists. *Mol Pharmacol* **45**(3): 490-499.

Cruickshank JM (1993). The xamoterol experience in the treatment of heart failure. *Am J Cardiol* **71**(9): 61C-64C.

Daaka Y, Luttrell LM, and Lefkowitz RJ (1997). Switching of the coupling of the beta2-adrenergic receptor to different G proteins by protein kinase A. *Nature* **390**(6655): 88-91.

Daaka Y, Luttrell LM, Ahn S, Della Rocca GJ, Ferguson SS, Caron MG and Lefkowitz RJ (1998). Essential role for G protein-coupled receptor endocytosis in the activation of mitogen-activated protein kinase. *J Biol Chem* **273**(2): 685-688.

Del Carmine R, Ambrosio C, Sbraccia M, Cotecchia S, Ijzerman AP and Costa T (2002). Mutations inducing divergent shifts of constitutive activity reveal different modes of binding among catecholamine analogues to the beta(2)-adrenergic receptor. *Br J Pharmacol* **135**(7): 1715-1722.

Dittman AH, Weber JP, Hinds TR, Choi EJ, Migeon JC, Nathanson NM, Storm DR (1994). A novel mechanism for coupling of m4 muscarinic acetylcholine receptors to calmodulin-sensitive adenylyl cyclases: crossover from G protein-coupled inhibition to stimulation. *Biochemistry*. **33**(4): 943-951.

Drake MT, Violin JD, Whalen EJ, Wisler JW, Shenoy SK, Lefkowitz RJ (2008). Beta-arrestin-biased agonism at the beta2-adrenergic receptor. *J Biol Chem* **283**(9): 5669-5676.

Ehlert FJ (2008). On the analysis of ligand-directed signaling at G protein-coupled receptors. *N-S Arch Pharmacol* **377**(4-6): 549-577.

Eichhorn EJ and Young JB (2001). Optimizing the use of beta-blockers in the effective treatment and management of heart failure: a case study approach. *Am J Med* **110 Suppl 5A**: 11S-20S.

Elster L, Elling C, Heding A (2007). Bioluminescence resonance energy transfer as a screening assay: Focus on partial and inverse agonism. *J Biomol Screen* **12**(1): 41-49.

Evans BA, Broxton N, Merlin J, Sato M, Hutchinson DS, Christopoulos A, and Summers RJ (2011). Quantification of functional selectivity at the human alpha(1A)-adrenoceptor. *Mol Pharmacol* **79**(2): 298-307.

Evans BA, Sato M, Sarwar M, Hutchinson DS, and Summers RJ (2010). Ligand-directed signaling at beta-adrenoceptors. *Br J Pharmacol* **159**(5): 1022-1038.

Ferguson-Myrthil N (2012). Vasopressor use in adult patients. *Cardiol Rev* **20**(3): 153-158.

Figuroa KW, Griffin MT, and Ehlert FJ (2009). Selectivity of agonists for the active state of M1 to M4 muscarinic receptor subtypes. *J Pharmacol Exp Ther*. 328(1):331-42.

Frielle T, Kobilka B, Lefkowitz RJ, and Caron MG (1988). Human beta 1- and beta 2-adrenergic receptors: structurally and functionally related receptors derived from distinct genes. *Trends Neurosci* **11**(7): 321-324.

Galandrin S and Bouvier M (2006). Distinct signaling profiles of beta1 and beta2 adrenergic receptor ligands toward adenylyl cyclase and mitogen-activated protein kinase reveals the pluridimensionality of efficacy. *Mol Pharmacol* **70**(5): 1575-1584.

Helfand M, Peterson K, and Dana T. (2007) Drug Class Review on Beta Adrenergic Blockers: Final Report [Internet]. Portland (OR): Oregon Health & Science University. <http://www.ncbi.nlm.nih.gov/books/NBK10440/>

Hoffmann C, Leitz MR, Oberdorf-Maass S, Lohse MJ, and Klotz KN (2004). Comparative pharmacology of human beta-adrenergic receptor subtypes--characterization of stably transfected receptors in CHO cells. *N-S Arch Pharmacol* **369**(2): 151-159.

Illarionov BA, Frank LA, Illarionova VA, Bondar VS, Vysotski ES, and Blinks JR (2000). Recombinant obelin: cloning and expression of cDNA purification, and characterization as a calcium indicator. *Method Enzymol* **305**: 223-249.

Isogaya M, Sugimoto Y, Tanimura R, Tanaka R, Kikkawa H, Nagao T, and Kurose H (1999). Binding pockets of the beta(1)- and beta(2)-adrenergic receptors for subtype-selective agonists. *Mol Pharmacol* **56**(5): 875-885.

Javed U and Deedwania PC (2009). Beta-adrenergic blockers for chronic heart failure. *Cardiol Rev* **17**(6): 287-292.

Keiper M, Stope MB, Szatkowski D, Bohm A, Tysack K, Vom Dorp F, Saur O, Oude-Weernink PA, Evellin S, Jakobs KH, and Schmidt M (2004). Epac- and Ca²⁺ -controlled activation of Ras and extracellular signal-regulated kinases by Gs-coupled receptors. *J Biol Chem* **279**(45): 46497-46508.

Kenakin T and Christopoulos A (2013). Signaling bias in new drug discovery: detection, quantification and therapeutic impact. *Nat Rev Drug Disc* **12**(3): 205-216.

Kenakin T, Watson C, Muniz-Medina V, Christopoulos A, Novick S (2012). A simple method for quantifying functional selectivity and agonist bias. *ACS Chem Neurosci* **3**(3): 193-203.

Liapakis G, Chan WC, Papadokostaki M, and Javitch JA (2004). Synergistic contributions of the functional groups of epinephrine to its affinity and efficacy at the beta2 adrenergic receptor. *Mol Pharmacol* **65**(5): 1181-1190.

McGraw DW, Almoosa KF, Paul RJ, Kobilka BK and Liggett SB (2003). Antithetic regulation by β -adrenergic receptors of Gq receptor signaling via phospholipase C underlies the airway β -agonist paradox. *J Clin Invest* **112**: 619-626.

McLean-Tooke AP, Bethune CA, Fay AC, and Spickett GP (2003). Adrenaline in the treatment of anaphylaxis:

what is the evidence? *Br Med J* **327**(7427): 1332-1335.

Moore RH, Millman EE, Godines V, Hanania NA, Tran TM, Peng H, *et al.* (2007). Salmeterol stimulation dissociates beta2-adrenergic receptor phosphorylation and internalization. *Am J Resp Cell Mol Biol* **36**(2): 254-261.

Pauwels PJ, Gommeren W, Van Lommen G, Janssen PA, and Leysen JE (1988). The receptor binding profile of the new antihypertensive agent nebivolol and its stereoisomers compared with various beta-adrenergic blockers. *Mol Pharmacol* **34**(6): 843-851.

Pauwels PJ, Van Gompel P, and Leysen JE (1991). Human beta 1- and beta 2-adrenergic receptor binding and mediated accumulation of cAMP in transfected Chinese hamster ovary cells. Profile of nebivolol and known beta-adrenergic blockers. *Biochem Pharmacol* **42**(9): 1683-1689.

Peng H, Bond RA, and Knoll BJ (2011). The effects of acute and chronic nadolol treatment on beta2AR signaling in HEK293 cells. *N-S Arch Pharmacol* **383**(2): 209-216.

Ponicke K, Heinroth-Hoffmann I, and Brodde OE (2002). Differential effects of bucindolol and carvedilol on noradrenaline-induced hypertrophic response in ventricular cardiomyocytes of adult rats. *J Pharmacol Exp Ther* **301**(1): 71-76.

Ponsioen B, Zhao J, Riedl J, Zwartkruis F, van der Krogt G, Zaccolo M, Moolenaar WH, Bos JL, and Jalink K. (2004). Detecting cAMP-induced Epac activation by fluorescence resonance energy transfer: Epac as a novel cAMP indicator. *EMBO reports* **5**(12): 1176-1180.

Rajagopal S, Ahn S, Rominger DH, Gowen-MacDonald W, Lam CM, Dewire SM, Violin JD, Lefkowitz RJ (2011). Quantifying ligand bias at seven-transmembrane receptors. *Mol Pharmacol* **80**(3): 367-377.

Ram CV (2010). Beta-blockers in hypertension. *Am J Cardiol* **106**(12): 1819-1825.

Rasmussen SG, Choi HJ, Rosenbaum DM, Kobilka TS, Thian FS, Edwards PC, Burghammer M, Ratnala VR, Sanishvili R, Fischetti RF, Schertler GF, Weis WI, and Kobilka BK (2007). Crystal structure of the human beta2 adrenergic G-protein-coupled receptor. *Nature* **450**(7168): 383-387.

Rasmussen SG, DeVree BT, Zou Y, Kruse AC, Chung KY, Kobilka TS, Thian FS, Chae PS, Pardon E, Calinski D, Mathiesen JM, Shah ST, Lyons JA, Caffrey M, Gellman SH, Steyaert J, Skinotitis G, Weis WI, Sunahara RK, and Kobilka BK (2011). Crystal structure of the beta2 adrenergic receptor-Gs protein complex. *Nature* **477**(7366): 549-555.

Reed SE, Staley EM, Mayginnes JP, Pintel DJ, and Tullis GE (2006). Transfection of mammalian cells using linear polyethylenimine is a simple and effective means of producing recombinant adeno-associated virus vectors. *J Virol Methods* **138**(1-2): 85-98.

Rovati GE and Nicosia S (1994). Lower efficacy: interaction with an inhibitory receptor or partial agonism? *Trends Pharmacol Sci.* **15**(5):140-144.

Schmidt M, Evellin S, Oude Weernink PA, vom Dorp F, Rehmann H, Lomasney JW and Jakobs KH (2001). A new phospholipase-C-calcium signaling pathway mediated by cyclic AMP and a Rap GTPase. *Nat Cell Biol.* **3**: 1020-1024.

Shenoy SK, Drake MT, Nelson CD, Houtz DA, Xiao K, Madabushi S, Reiter E, Premont RT, Lichtarge O, and Lefkowitz RJ (2006). Beta-arrestin-dependent, G protein-independent ERK1/2 activation by the beta2 adrenergic receptor. *J Biol Chem* **281**(2): 1261-1273.

Smart NA, Kwok N, Holland DJ, Jayasighe R, and Giallauria F (2011). Bucindolol: a pharmacogenomic perspective on its use in chronic heart failure. *Clin Med Insights. Cardiol* **5**: 55-66.

- Tzingounis AV, von Zastrow M, Yudowski GA (2010). β -blocker drugs mediate calcium signaling in native central nervous system neurons by β -arrestin-biased agonism. *Proc Natl Acad Sci U S A*. **107**(49): 21028-33.
- U'Prichard DC, Bylund DB, and Snyder SH (1978). (+/-)-[3H]Epinephrine and (-)[3H]dihydroalprenolol binding to beta1- and beta2-noradrenergic receptors in brain, heart, and lung membranes. *J Biol Chem* **253**(14): 5090-5102.
- Violin JD, DiPilato LM, Yildirim N, Elston TC, Zhang J, and Lefkowitz RJ (2008). Beta2-adrenergic receptor signaling and desensitization elucidated by quantitative modeling of real time cAMP dynamics. *J Biol Chem* **283**(5): 2949-2961.
- Violin JD, Soergel DG, Boerrigter G, Burnett JC Jr, Lark MW (2013). GPCR biased ligands as novel heart failure therapeutics. *Trends Cardiovasc Med* **23**(7):242-9
- Wacker D, Fenalti G, Brown MA, Katritch V, Abagyan R, Cherezov V, and Stevens RC (2010). Conserved binding mode of human beta2 adrenergic receptor inverse agonists and antagonist revealed by X-ray crystallography. *J Am Chem Soc* **132**(33): 11443-11445.
- Wisler JW, DeWire SM, Whalen EJ, Violin JD, Drake MT, Ahn S, Shenoy SK and Lefkowitz RJ (2007). A unique mechanism of beta-blocker action: carvedilol stimulates beta-arrestin signaling. *Proc Nat Acad Sci USA* **104**(42): 16657-16662.
- Zhang ZS, Cheng HJ, Ukai T, Tachibana H and Cheng CP (2001). Enhanced cardiac L-type calcium current response to β 2-adrenergic stimulation in heart failure. *J Pharmacol Exp Ther*. **298**: 188-196
- Zimmerman B, Beaudrait A, Aguila B, Charles R, Escher E, Claing A, Bouvier M, and Laporte SA (2012). Differential beta-arrestin-dependent conformational signaling and cellular responses revealed by angiotensin analogs. *Science signal* **5**(221): ra33.

Footnotes:

- a) This work was supported, in part, by the grants to MB from the Canadian Institutes for Health Research [MOP 11215]. ETvdW was supported by post-doctoral research fellowships from the Canadian Institutes for Health Research, the Canadian Hypertension Society, the Fonds de la Recherche en Santé du Québec and the National Health and Medical Research Council Australia (NHMRC). BB was supported by a PhD scholarship from the Fonds de la Recherche en Santé du Québec. AC is a Principal Research Fellow of the NHMRC. MB holds the Canada Research Chair in Signal Transduction and Molecular Pharmacology.
- b)
- c) Reprint requests to Dr. Michel Bouvier. IRIC-Université de Montréal C.P. 6128 Succursale Centre-Ville Montréal, Québec H3C 3J7 Canada. michel.bouvier@umontreal.ca
- d) ¹Due to model parameter redundancy, it is usually not possible to estimate *separate* τ or K_A values for full agonists from direct fitting of the operational model to a full agonist concentration-response curve unless additional experimental manipulations are performed to provide information about other model parameters (e.g., receptor alkylation studies to reduce system maximum responsiveness and thus allow estimation of E_m), or parameter values are constrained to prior known values. However, the τ/K_A ratio, as a single fitted parameter ('R' in the formulation used herein), can still be estimated from full agonist concentration-response curves as it is obtained from the EC_{50} of the full agonist curve. Specifically, in operational model terms, the $EC_{50} = K_A / ((2 + \tau^n)^{1/n} - 1)$ (Black et al., 1985). For high efficacy agonists (high τ values), this reduces to $K_A / (\tau^n)^{1/n}$. If the transducer slope, n , equals 1, then the τ/K_A ratio is simply the reciprocal of the full agonist's EC_{50} value. Constraining the LogKA parameter in the operational model equation to an arbitrarily low "dummy" value, such as zero, ensures convergence of full agonist data to the correct τ/K_A ratio (i.e., LogR parameter).

Figure Legends:

Figure 1 – Selective adrenoceptor antagonists differentially block the EC₅₀₋₈₀ of clinically relevant ligands toward the four signaling outcomes. Cells were pre-treated (1h, 37°C) with selective adrenoceptor antagonists, CGP-20712A (β 1AR; 100nM), ICI 118,551 (β 2AR; 100nM), prazosin (α 1AR; 10nM) or rauwolscine (α 2AR; 100nM) then treated with ISO (100nM cAMP; 10nM ERK1/2, 1 μ M calcium, 10 μ M endocytosis), EPI (3 μ M cAMP; 10 μ M ERK1/2, 10 μ M calcium; 10 μ M endocytosis), NE (3 μ M cAMP; 3 μ M ERK1/2; 10 μ M calcium, 10 μ M endocytosis), SALB (1nM cAMP; 0.1nM ERK1/2, 10 μ M calcium, 10 μ M endocytosis), SALM (100nM cAMP; 3nM ERK1/2; 10 μ M calcium), LAB (3nM cAMP; 1nM ERK1/2), ALP (1nM cAMP; 3nM ERK1/2), BUC (30nM cAMP; 10nM ERK1/2), PIN (10 μ M cAMP; 10nM ERK1/2), XAM (1 μ M ERK1/2), CARV (30nM ERK1/2), PRO (100nM ERK1/2), NEB (1 μ M cAMP), ATEN (10 μ M cAMP), TIM (1 μ M cAMP), BET (10 μ M cAMP), MET (10 μ M cAMP), BIS (10 μ M cAMP), NAD (10 μ M cAMP) (37°C). Responses were measured toward cAMP (30 min), ERK1/2 (2-4 min), calcium (0-60 sec) and receptor endocytosis (30 min) following stimulation with test compounds. Data are the mean \pm standard error of the mean of 4-6 independent experiments with repeats in duplicate. The data were analyzed by one way ANOVA with a Dunnett post hoc test (comparing to the effect of the compound alone), where a is $p < 0.05$ for cAMP, b is $p < 0.05$ for ERK1/2, c is $p < 0.05$ for calcium and d is $p < 0.05$ for receptor endocytosis.

Figure 2 – Increasing concentrations of the β 2AR-selective antagonist, ICI 118,551, shifts the agonist-stimulated concentration-response curves of cAMP. Pre-treating cells with ICI 118,551 (10nM or 1 μ M; 60 min) right-shifted the concentration-response curves of the β 2AR-selective ligands ISO (A), SALB (B), SALM (C), LAB (D), BUC (E), PIN (F) in a classically competitive manner. Data are the mean \pm SEM of 5 independent experiments performed in triplicate.

Figure 3 – Increasing concentrations of the β 2AR-selective antagonist, ICI 118,551, shifts the agonist-stimulated concentration-response curves of ERK1/2. Pre-treating cells with ICI 118,551 (10nM or 1 μ M; 60 min) right-shifted the concentration-response curves of the β 2AR-selective ligands ISO (A), SALB (B), SALM (C),

LAB (D), BUC (E), PIN (F), XAM (G), CARV (H). Data are the mean \pm standard error of the mean of 5 independent experiments performed in triplicate.

Figure 4 – Increasing concentrations of the β 2AR-selective antagonist, ICI 118,551, shifts the agonist-stimulated concentration-response curves of calcium. Pre-treating cells with ICI 118,551 (10nM or 1 μ M; 60 min) right-shifted the concentration-response curves of the β 2AR-selective ligands ISO (A), SALB (B) and SALM (C). Data are the mean \pm standard error of the mean of 3 independent experiments with repeats in triplicate.

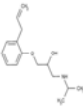
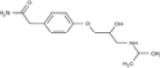
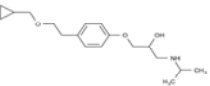
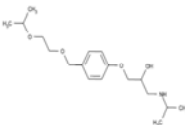
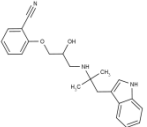
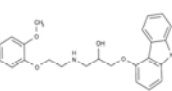
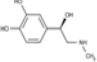
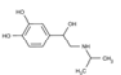
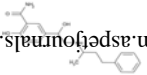
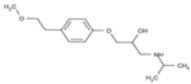
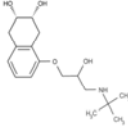
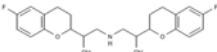
Figure 5 – Increasing concentrations of the β 2AR-selective antagonist, ICI 118,551, shifts the agonist-stimulated concentration-response curves for receptor endocytosis. Pre-treating cells with ICI 118,551 (10nM or 1 μ M; 60 min) right-shifted the concentration-response curves of the β 2AR-selective ligands ISO (A) and SALB (B). Data are the mean \pm standard error of the mean of 3 independent experiments with repeats in triplicate.

Figure 6 – Increasing concentrations of the β 2AR-selective antagonist, ICI 118,551, did not shift the inverse agonist-stimulated concentration-response curves of cAMP. Pre-treating cells with ICI 118,551 (10nM or 1 μ M; 60 min) did not shift the concentration-response curves for NAD (A) or BET (B), which were identified as inverse agonists toward cAMP, due to the inverse agonist activity of ICI 118,551 that itself decreased the cAMP levels following pre-treatment of the cells (60 min). Data are the mean \pm standard error of the mean of 4-6 independent experiments performed in triplicate.

Figure 7 – The profiles of the adrenergic ligands fall into 5 distinct clusters based on their efficacy and potency toward the 4 different signaling pathways. Cells were stimulated with increasing concentrations of ISO (A), SALB (B), SALM (C), LAB (D), BUC (E), PIN (F), XAM (G), CARV(H), BIS (I) and NAD (J). Responses to the different signaling pathways were measured: cAMP using EPAC biosensor (37°C; 30 min), ERK1/2 with the Surefire pERK1/2 kit (37°C; 2 or 4 min), calcium with the obelin biosensor (25°C, 0-60 sec) and receptor internalization by cell surface ELISA (37°C, 30 min). Data are the mean \pm standard error of the mean of 3-6 independent experiments with repeats in triplicate.

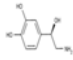
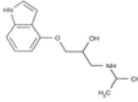
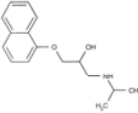
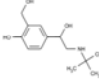
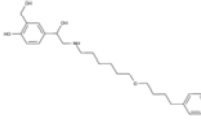
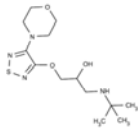

Figure 8 – Adrenergic ligands are predominantly biased toward ERK1/2 signaling. Bias factors were calculated from the agonist concentration-response curves (shown in figure 7) using the operational model (see Appendix 1). The $\Delta\Delta\text{Log}(\tau/K_A)$ value is indicated on top of the bars. Log(bias factor) of the ligands demonstrate that SALB (purple bars), SALM (red bars) and LAB (light blue bars) were strongly biased toward the ERK1/2 pathway over all other pathways. BUC (yellow bar) and PIN (orange bar) were not biased toward either the ERK1/2 or cAMP signaling. There was no bias observed between the calcium and endocytosis for SALB. Data are the mean of 3-6 independent experiments with repeats in duplicate or triplicate.

Table 1 – Clinically relevant compounds selected for the study. The 19 adrenergic compounds initially selected for this study are listed in alphabetical order. Their binding affinities (pK_D) toward the β2AR were determined using [¹²⁵I]-cyanopindolol, [¹²⁵I]-pindolol or [³H]-CGP-12177A in cell lines overexpressing the β2AR or in tissues endogenously expressing the β2AR. The potencies (pEC₅₀) of these compounds toward cAMP signaling, is also shown. The compound structures, their selectivity for the different adrenergic receptor subtypes and their clinical uses are also indicated.

Compound	pK _D (range)	pEC ₅₀ (range)	Compound Structure	Classification	Clinical uses
Alprenolol	8.92-9.11 ^{1, 5, 7}	↑ 9.08 ¹⁴ ↓ 8.17 ¹⁸		Non-selective βAR antagonist	Hypertension, angina, arrhythmia.
S(-)-Atenolol	5.08 - 5.99 ^{1, 5}	↓ 5.62-6.63 ^{14, 15}		Selective β1AR antagonist	Hypertension, chronic stable angina, ischemic heart disease (IHD), post-myocardial infaction ^{9, 10, 12}
Betaxolol	7.38 ¹	NT		Selective β1AR antagonist	Hypertension, Glaucoma ^{9, 10, 12}
Bisoprolol	5.94 - 6.70 ^{1, 5, 7}	↓ 6.51-6.70 ^{14, 15}		Selective β1AR antagonist	Hypertension, angina, IHD, heart failure ^{9, 12}
Bucindolol	8.92 ^{6, 8}	↑ 9.40 ⁸ > 5.00 ¹⁵		Non-selective βAR antagonist	Heart failure ²¹
Carvedilol	9.02 – 9.40 ^{1, 5, 6}	↑ 9.10 ¹⁴ >5.00 ¹⁵		α1AR and βAR antagonist	Hypertension, IHD, heart failure, post-MI ^{9, 10, 12}
(-)-Epinephrine	5.99- 6.54 ^{4, 5, 7, 8}	↑ 7.74 – 8.22 ^{8, 13, 17}		Non-selective endogenous αAR and βAR agonist	Allergic reactions, asthma, cardiac failure, hemorrhage, shock ¹¹ , hypotension ²⁴
(-)-Isoproterenol	6.34 – 7.54 ^{4, 5, 7, 8}	↑ 7.60 – 9.25 ^{8, 13, 15, 16, 18}		Non-selective βAR agonist	Allergic reaction, bronchodilation and heart stimulant.
Labetalol	7,71 - 8.03 ^{1, 2, 7}	↑ 8.08 – 8.17 ^{14, 15} ↓ 7.21 ¹⁸		α1AR and βAR antagonist	Hypertension, hypertensive emergencies ^{9, 10, 12}
(±)-Metoprolol	5.52 - 6.89 ^{1, 5}	↓ 6.53 – 7.22 ^{14, 15}		Selective β1AR antagonist	Angina, hypertension, heart failure, post-MI, IHD, migraine ^{9, 12}
Nadolol	8.60 ¹	↓ ²⁰		Non-selective βAR antagonist	Hypertension, IHD, arrhythmias, migraine, thyrotoxicosis, angina ^{9, 12}
Nebivolol	7.31 - 7.92 ^{2, 8}	NR ⁸ – ↓ 7.05 ²¹		Selective β1AR antagonist, also	Hypertension, heart failure ^{10, 12}

Molecular Pharmacology Fast Forward. Published on December 23, 2013 as DOI: 10.1124/mol.113.088880
This article has not been certified and formatted. The final version may differ from this version.

Downloaded from molpharm.aspetjournals.org at ASPET Journals on April 9, 2024

				activates nitric oxide pathway.	
(-)-Norepinephrine	4.19 – 5.41 ^{4, 5, 7, 8}	↑5.61 – 7.46 ^{8, 13, 17}		Non-selective endogenous αAR and βAR agonist	Severe hypotension ²⁴
Pindolol	8.32 – 9.32 ^{2, 5, 7, 8}	↑ 8.96±0.06 ¹⁴ ↓ 7.44±0.08 ¹⁸		Non-selective βAR antagonist	Hypertension ⁹
(±)-Propranolol	9.08 – 9.37 ^{1, 5, 6, 7}	↓ 8.10 – 9.17 ^{14, 15}		Non-cardioselective βAR antagonist	Hypertension, angina, atrial arrhythmia, portal hypertension, anxiety, tremor, thyrotoxicosis, migraine ^{9, 12}
Salbutamol	5.66 – 6.42 ^{1, 5, 7, 8}	↑ 7.10 – 7.72 ^{8, 13}		Selective β2AR agonist	Asthma, chronic obstructive pulmonary disease ¹⁹
Salmeterol	7.61 – 9.26 ^{1, 5, 8}	↑ 8.74 – 9.89 ^{8, 13}		Selective β2AR agonist	Asthma, chronic obstructive pulmonary disease, allergy ¹⁹
Timolol	9.68 ¹	↓ 8.00 – 8.89 ^{14, 18}		Non-selective βAR antagonist.	Hypertension, glaucoma, IHD, migraine, post-MI ^{9, 12}
Xamoterol	5.55 - 6.07 ^{1, 3, 7}	↑ ⁷		Selective β1AR partial agonist	Myocardial ischemia, mild-moderate heart failure ²³ .

References: ¹(Baker et al., 2005); ²(Pauwels et al., 1988); ³(Isogaya et al., 1999); ⁴(Frielle et al., 1988); ⁵(Hoffman et al., 2004); ⁶(Ponicke et al., 2002); ⁷(Del Carmine et al, 2003); ⁸(Baker, 2010); ⁹(Helfand et al., 2007); ¹⁰(Ram, 2010); ¹¹(McLean-Tooke, 2003) ¹²(Baker et al., 2011); ¹³(Elster et al., 2007); ¹⁴(Baker et al., 2003); ¹⁵(Galandrin and Bouvier, 2006); ¹⁹(Violin et al., 2008); ¹⁷(Liapakis et al., 2004); ¹⁸(Chidiac et al., 1994); ¹⁹(Castle et al., 1993); ²⁰(Peng et al., 2011); ²¹(Pauwels et al., 1991); ²²(Smart et al., 2011); ²³(Cruickshank, 1993); ²⁴(Ferguson-Myrthil, 2012)

Table 2 – Potencies, relative efficacies (E_{\max}) and kinetics of activation of cAMP, ERK1/2, calcium signaling pathways and receptor endocytosis by adrenergic ligands. HEK-HA- β 2AR cells were stimulated with different concentrations of clinically relevant adrenergic ligands and responses were measured for 4 distinct signaling pathways (cAMP, 30min; ERK1/2, 2 or 4 min; calcium 0-60 sec and endocytosis 30 min). The negative pEC_{50} values reported for some ligands mean that the curve was biphasic, and these are the pEC_{50} values for the part of the curve following the E_{\max} . Data are the mean \pm standard error of the mean of 4-6 independent experiments with repeats in duplicate.

Ligand	cAMP			pERK1/2			Ca ²⁺			Endocytosis		
	pEC_{50}	E_{\max}	$t_{1/2}$ (min)	pEC_{50}	E_{\max}	Peak	pEC_{50}	E_{\max}	Peak	pEC_{50}	E_{\max}	$t_{1/2}$ (min)
		(%ISO)			(%ISO)	(min)		(%ISO)	(sec)		(%ISO)	
ISO*	8.23 \pm 0.15	100	2.54 \pm 0.18	7.95 \pm 0.13	100	4	7.47 \pm 0.21	100	18.0 \pm 1.08	7.88 \pm 0.26	100	7.64 \pm 0.04
EPI	7.78 \pm 0.23	74.04 \pm 6.19	1.64 \pm 0.05	6.79 \pm 0.19	157.7 \pm 14.13	2	6.82 \pm 0.08	112.0 \pm 4.10	17.4 \pm 0.87	7.26 \pm 0.16	115.5 \pm 6.24	12.26 \pm 0.02
NE	7.08 \pm 0.25	88.32 \pm 8.53	1.74 \pm 0.16	6.48 \pm 0.12	154.6 \pm 9.26	2	6.21 \pm 0.24	58.01 \pm 9.43	21.7 \pm 1.32	5.64 \pm 0.30	90.00 \pm 12.5	12.40 \pm 0.04
SALB*	9.08 \pm 0.31	111.3 \pm 10.5	2.29 \pm 0.12	10.81 \pm 0.28	87.16 \pm 5.89	2	7.72 \pm 0.28	50.93 \pm 4.50	19.8 \pm 0.46	5.93 \pm 0.31	44.94 \pm 6.86	5.62 \pm 0.34
SALM*	8.63 \pm 0.20	105.5 \pm 6.11	1.94 \pm 0.14	10.14 \pm 0.23	74.39 \pm 5.28	2	5.80 \pm 0.39	34.45 \pm 6.10	30.9 \pm 2.86	>4.00	NR	NR
LAB*	7.82 \pm 0.23	51.84 \pm 3.73	2.61 \pm 0.38	10.28 \pm 0.28	111.9 \pm 7.52	4	>4.00	NR	NR	>4.00	NR	NR
BUC*	8.64 \pm 0.38	62.07 \pm 7.48	2.45 \pm 0.16	8.51 \pm 0.41	107.2 \pm 22.1	2	>4.00	NR	NR	>4.00	NR	NR
				-4.86 \pm 0.26								
ALP	9.81 \pm 0.39	35.76 \pm 3.70	2.64 \pm 0.61	9.54 \pm 0.28	102.3 \pm 5.71	4	>4.00	NR	NR	>4.00	NR	NR
				-6.63 \pm 0.34								
PIN*	9.50 \pm 0.49	18.43 \pm 2.51	0.96 \pm 0.14	8.90 \pm 0.48	81.55 \pm 19.86	4	>4.00	NR	NR	>4.00	NR	NR
				-5.76 \pm 0.34								
XAM*	>4.00	NR	NR	6.58 \pm 0.22	102.7 \pm 8.63	4	>4.00	NR	NR	>4.00	NR	NR

PRO	>4.00	NR	NR	7.87±0.13	77.28±7.18	4	>4.00	NR	NR	>4.00	NR	NR
				-5.79±0.44								
CARV*	>4.00	NR	NR	7.98±0.12	88.55±12.47	4	>4.00	NR	NR	>4.00	NR	NR
				-5.68±0.35								
ICI	7.95±0.45	-35.46±5.39	14.15±0.13	>4.00	NR	NR	>4.00	NR	NR	>4.00	NR	NR
BIS	6.96±0.77	-18.25±5.04	6.50±1.01	>4.00	NR	NR	>4.00	NR	NR	>4.00	NR	NR
BET*	6.75±0.42	-39.80±10.8	5.42±2.69	>4.00	NR	NR	>4.00	NR	NR	>4.00	NR	NR
MET	6.87±0.55	-39.00±9.46	6.68±2.46	>4.00	NR	NR	>4.00	NR	NR	>4.00	NR	NR
NEB	7.46±0.57	-13.79±4.04	17.48±3.94	>4.00	NR	NR	>4.00	NR	NR	>4.00	NR	NR
NAD*	8.24±0.37	-34.07±7.80	3.48±1.57	>4.00	NR	NR	>4.00	NR	NR	>4.00	NR	NR
ATEN	5.44±0.44	-49.38±10.9	7.77±1.99	>4.00	NR	NR	>4.00	NR	NR	>4.00	NR	NR
TIM	8.81±0.40	-44.45±5.28	4.47±0.11	>4.00	NR	NR	>4.00	NR	NR	>4.00	NR	NR

* indicates the compounds that were selectively signaling via the β2AR.

Table 3 – Transduction ratios ($\log(\tau/K_A)$) of adrenergic agonists at the $\beta 2AR$. HEK-HA- $\beta 2AR$ cells were stimulated with different concentrations of $\beta 2AR$ -selective ligands and responses were measured for 4 distinct signaling pathways. Data were analyzed by non-linear regression using the Operational Model equation (see appendix 1) in Graphpad Prism v6 to determine the LogR values (equivalent to $\log(\tau/K_A)$ ratios). $\Delta\log(\tau/K_A)$ ratios were calculated from the $\log(\tau/K_A)$ ratios considering ISO as the reference ligand using equation 8. The relative effectiveness (RE) of the ligands toward each pathway, relative to ISO, was determined by equation 9. The standard error was estimated using equation 13. Data are the mean \pm standard error of the mean of 3-6 independent experiments with repeats in duplicate. Data were analyzed in a pairwise manner using a two-tailed unpaired student's t-test (on the $\Delta\log(\tau/K_A)$ ratios) to determine the significance of the relative effectiveness.

Ligand	cAMP			ERK1/2			Ca ²⁺			Endocytosis		
	Log(τ/K_A)	$\Delta\log(\tau/K_A)$	RE	Log(τ/K_A)	$\Delta\log(\tau/K_A)$	RE	Log(τ/K_A)	$\Delta\log(\tau/K_A)$	RE	Log(τ/K_A)	$\Delta\log(\tau/K_A)$	RE
ISO	7.65 \pm 0.15	0.00 \pm 0.22	1.00	7.37 \pm 0.19	0.00 \pm 0.27	1.00	7.00 \pm 0.27	0.00 \pm 0.39	1.00	7.24 \pm 0.16	0.00 \pm 0.23	1.00
SALB	8.77 \pm 0.31	1.13 \pm 0.35	13.40*	10.29 \pm 0.34	2.92 \pm 0.39	829.91*	7.66 \pm 0.36	0.66 \pm 0.46	4.54	7.81 \pm 0.28	0.57 \pm 0.32	3.73
SALM	8.74 \pm 0.17	1.09 \pm 0.23	12.29*	9.74 \pm 0.29	2.37 \pm 0.35	233.98*	6.87 \pm 0.26	-0.13 \pm 0.38	0.74	ND	ND	ND
LAB	8.24 \pm 0.29	0.59 \pm 0.33	3.89	11.01 \pm 0.03	3.63 \pm 0.20	4307.91*	ND	ND	ND	ND	ND	ND
PIN	8.50 \pm 0.82	0.85 \pm 0.84	7.08	7.41 \pm 0.03	0.04 \pm 0.20	1.09	ND	ND	ND	ND	ND	ND
BUC	8.11 \pm 0.07	0.46 \pm 0.17	2.87*	7.35 \pm 0.10	-0.02 \pm 0.22	0.96	ND	ND	ND	ND	ND	ND
XAM	ND	ND	ND	8.39 \pm 0.48	1.02 \pm 0.52	10.47	ND	ND	ND	ND	ND	ND
CARV	ND	ND	ND	6.05 \pm 0.08	-1.32 \pm 0.21	0.05*	ND	ND	ND	ND	ND	ND

Where ND means not determined. * $p < 0.05$

Table 4 – $\Delta\Delta\log(\tau/K_A)$ ratios and bias factors for adrenergic agonists at the β_2 AR. HEK-HA- β_2 AR cells were stimulated with different concentrations of clinically relevant β_2 AR-selective ligands and responses were measured for 4 distinct signaling pathways. $\Delta\Delta\log(\tau/K_A)$ ratios were calculated from the $\Delta\log(\tau/K_A)$ ratios (Table 3) using equation 10. The ligand bias factors (BF), relative to ISO, were determined using equation 11. The standard error was estimated using equation 14. Data are the mean \pm standard error of 3-6 independent experiments with repeats in duplicate. Data were analyzed in a pairwise manner using a two-tailed unpaired student's t-test (on the $\Delta\log(\tau/K_A)$ ratios) to determine the significance of the ligand biases.

Ligand	ERK1/2-cAMP		ERK1/2-Ca ²⁺		cAMP-Ca ²⁺		Ca ²⁺ -Endocytosis		cAMP-Endocytosis		ERK1/2-Endocytosis	
	$\Delta\Delta\log(\tau/K_A)$	BF	$\Delta\Delta\log(\tau/K_A)$	BF	$\Delta\Delta\log(\tau/K_A)$	BF	$\Delta\Delta\log(\tau/K_A)$	BF	$\Delta\Delta\log(\tau/K_A)$	BF	$\Delta\Delta\log(\tau/K_A)$	BF
ISO	0.00 \pm 0.34	1.00	0.00 \pm 0.48	1.00	0.00 \pm 0.44	1.00	0.00 \pm 0.45	1.00	0.00 \pm 0.32	1.00	0.00 \pm 0.35	1.00
SALB	1.79 \pm 0.52	61.92*	2.26 \pm 0.60	182.89*	0.47 \pm 0.57	2.95	0.09 \pm 0.56	1.22	0.56 \pm 0.48	3.60	2.35 \pm 0.50	222.73*
SALM	1.28 \pm 0.42	19.03*	2.50 \pm 0.51	315.56*	1.22 \pm 0.44	16.58*	ND	ND	ND	ND	ND	ND
LAB	3.04 \pm 0.0.38	1108.07*	ND	ND	ND	ND	ND	ND	ND	ND	ND	ND
BUC	-0.48 \pm 0.0.27	0.33	ND	ND	ND	ND	ND	ND	ND	ND	ND	ND
PIN	-0.81 \pm 0.86	0.15	ND	ND	ND	ND	ND	ND	ND	ND	ND	ND

Where ND means not determined due to lack of a concentration-response curve at the concentrations of the ligand tested. *p<0.05

FIGURE 1

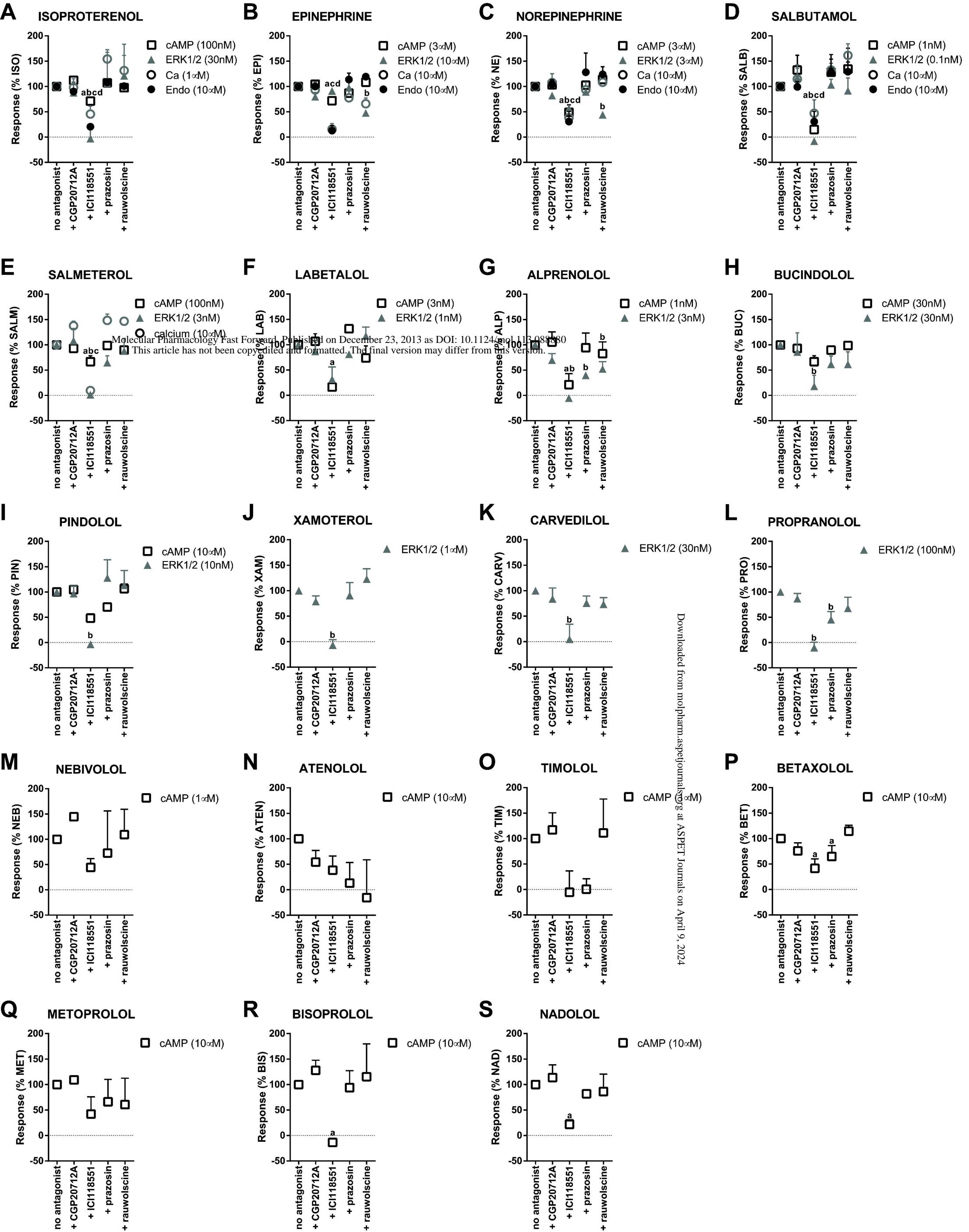


FIGURE 2

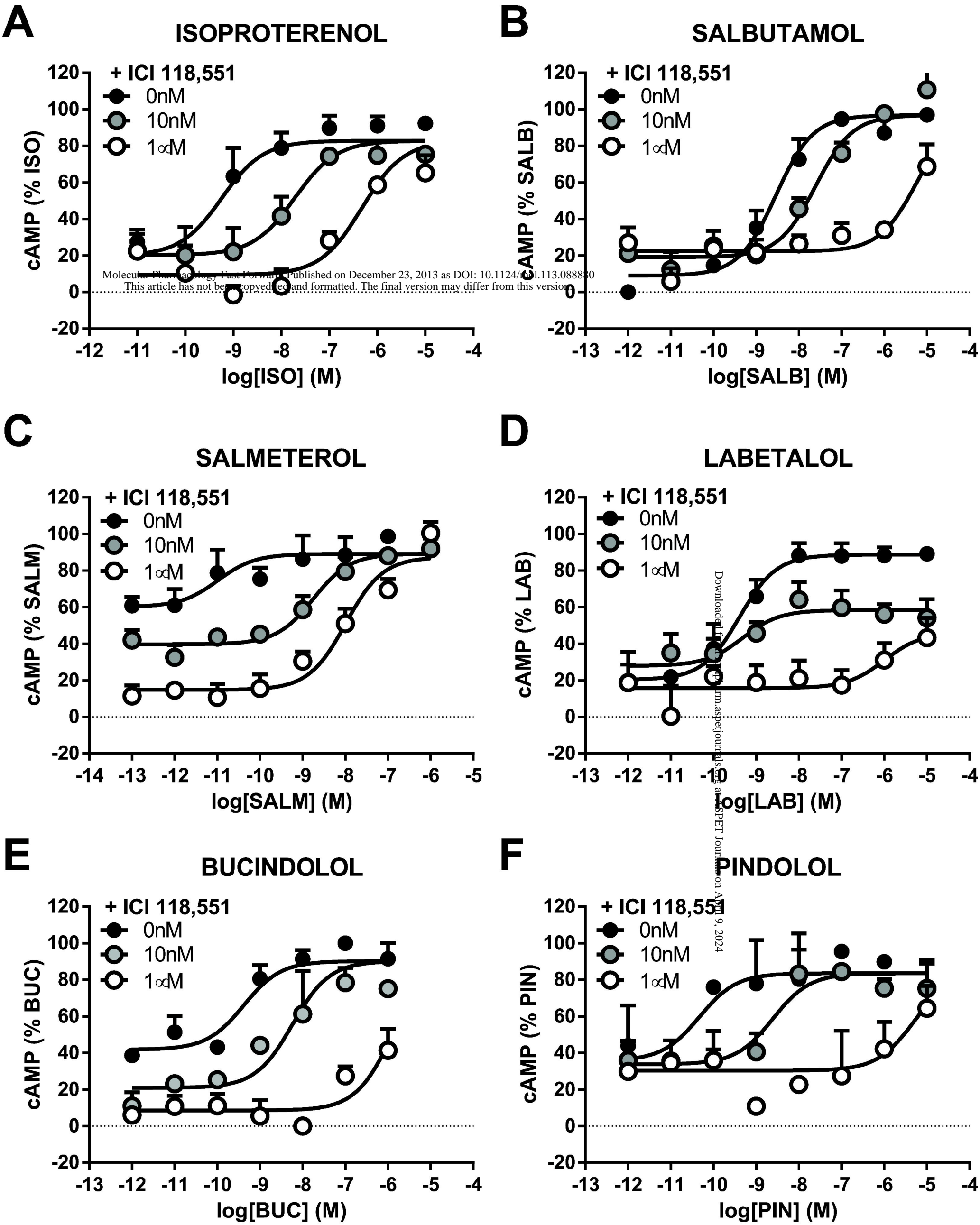


FIGURE 3

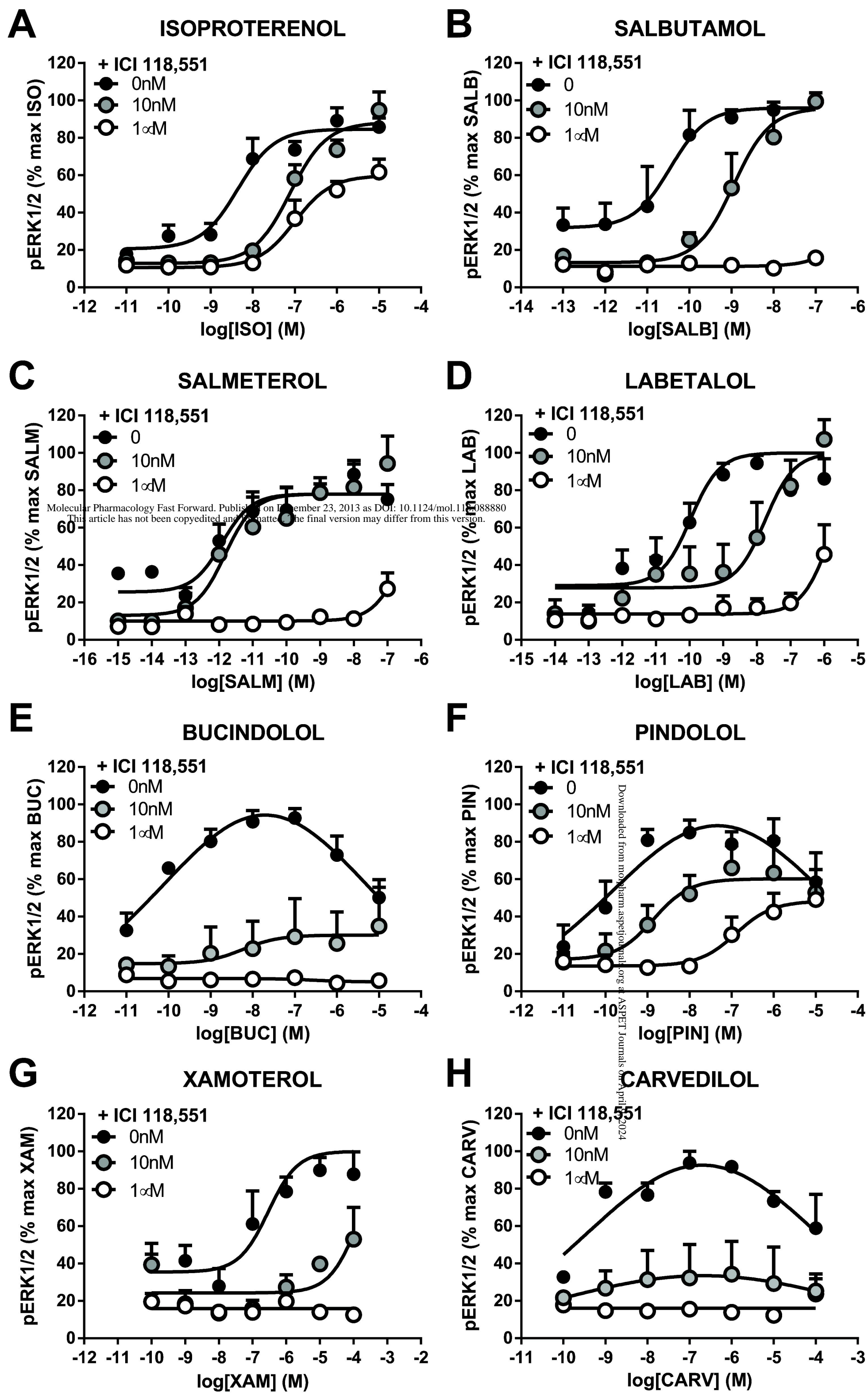
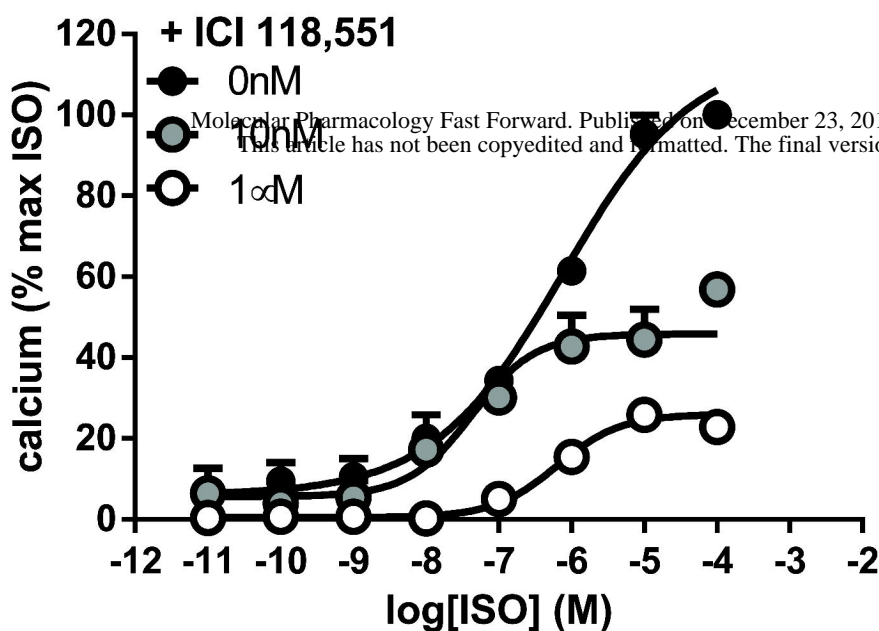


FIGURE 4

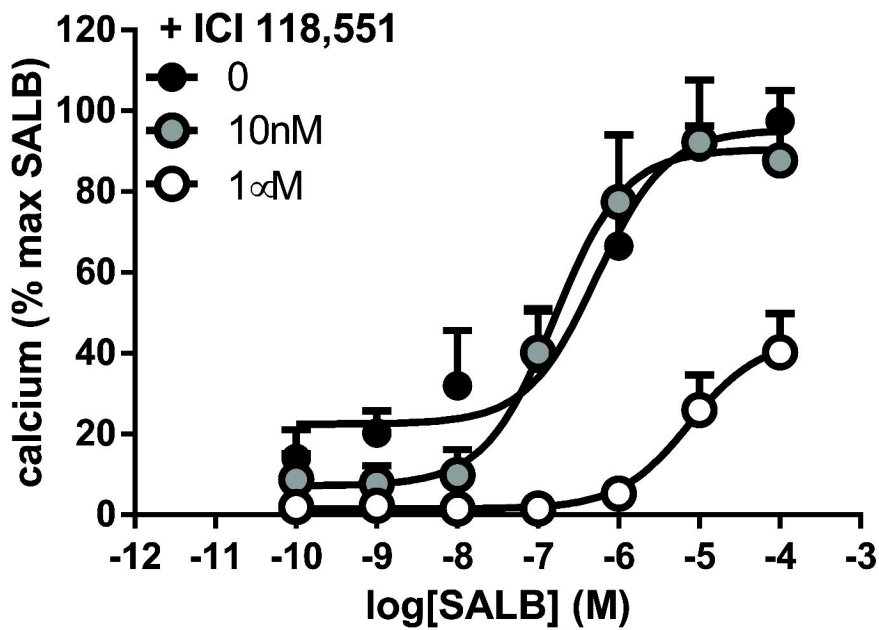
A

ISOPROTERENOL



B

SALBUTAMOL



C

SALMETEROL

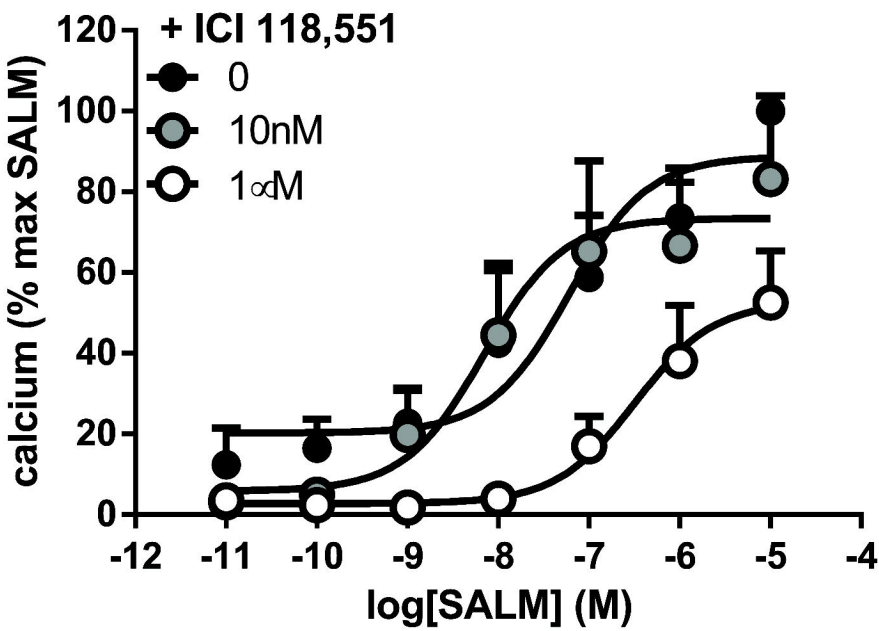
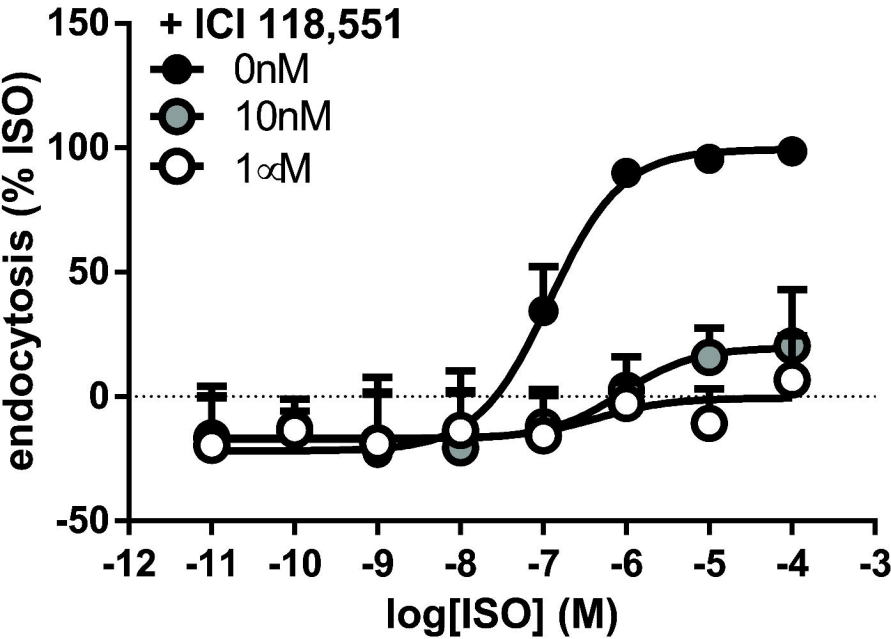


FIGURE 5

A ISOPROTERENOL



B SALBUTAMOL

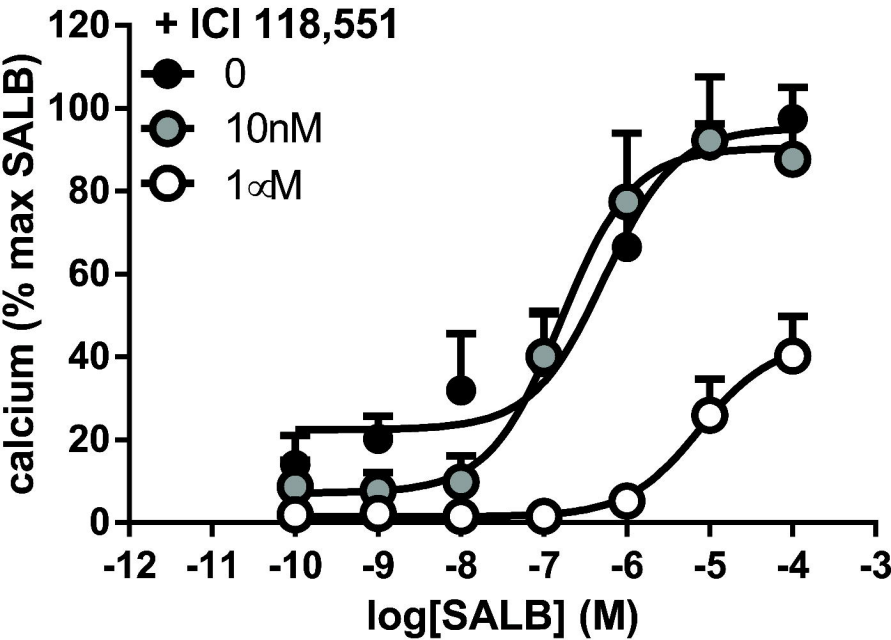
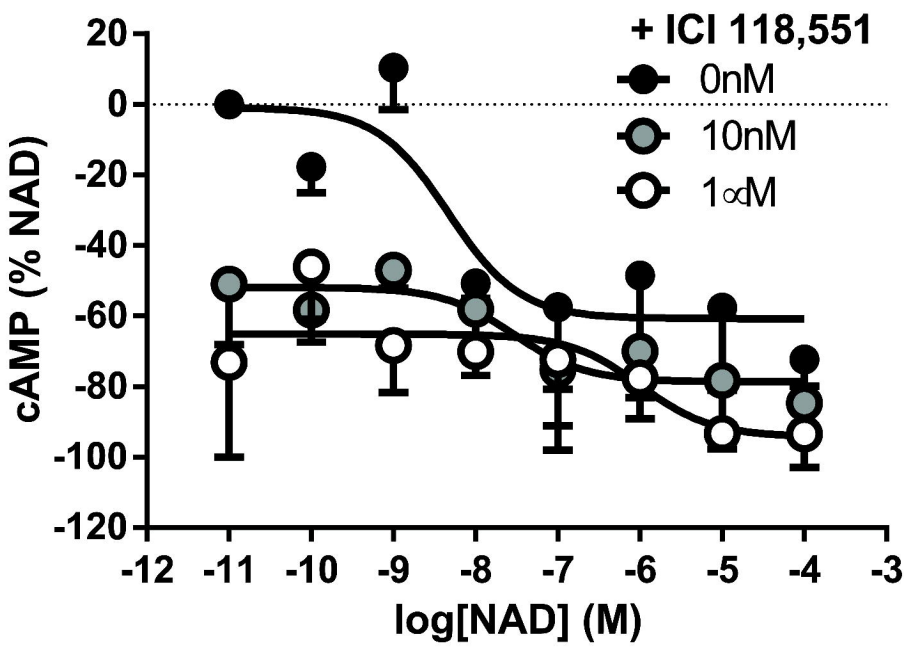


FIGURE 6

A

NADOLOLOL



B

BETAXOLOL

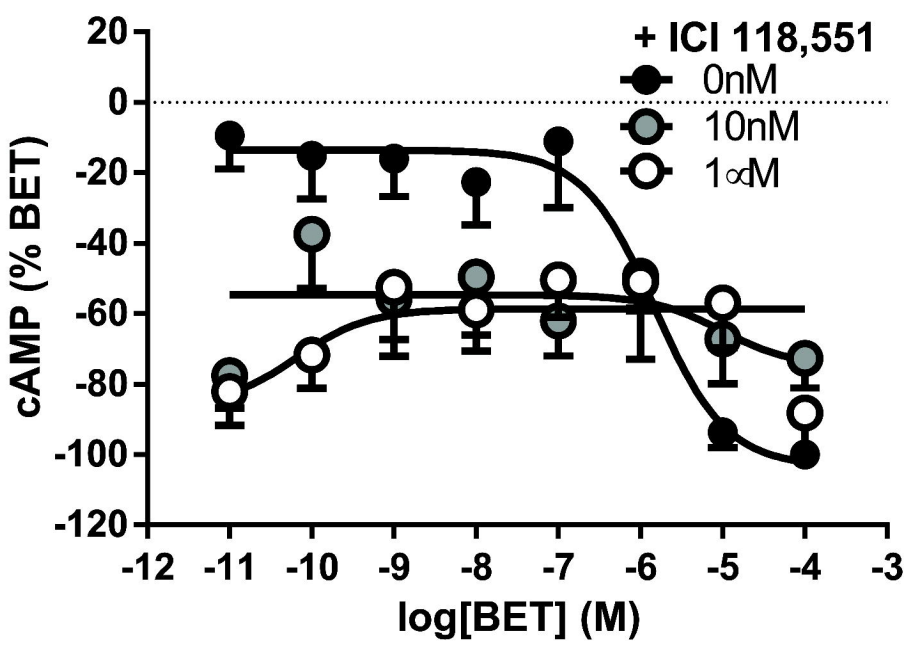
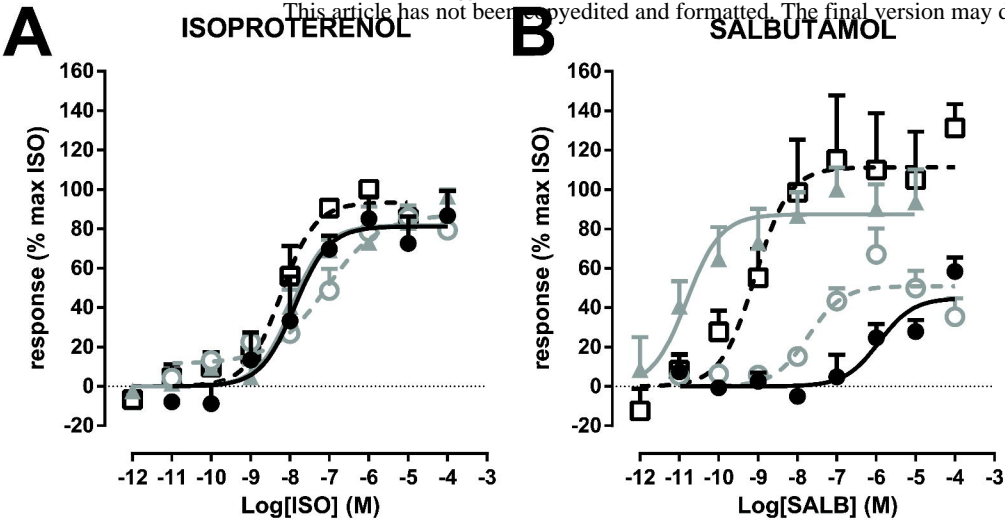


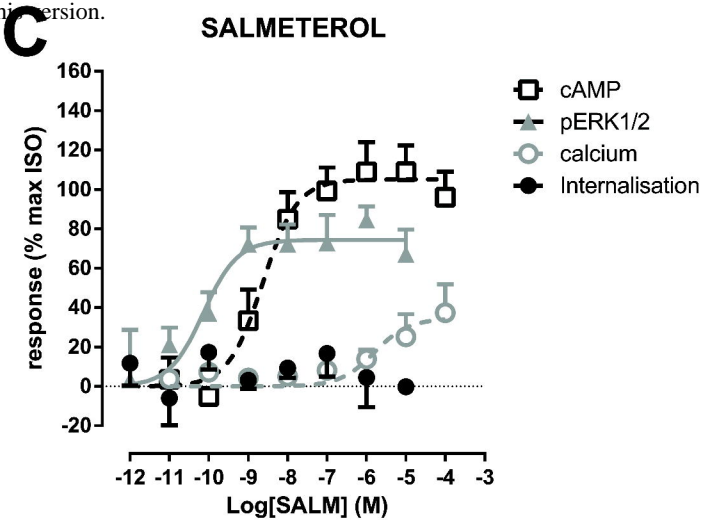
FIGURE 7

Group I: 4 pathways

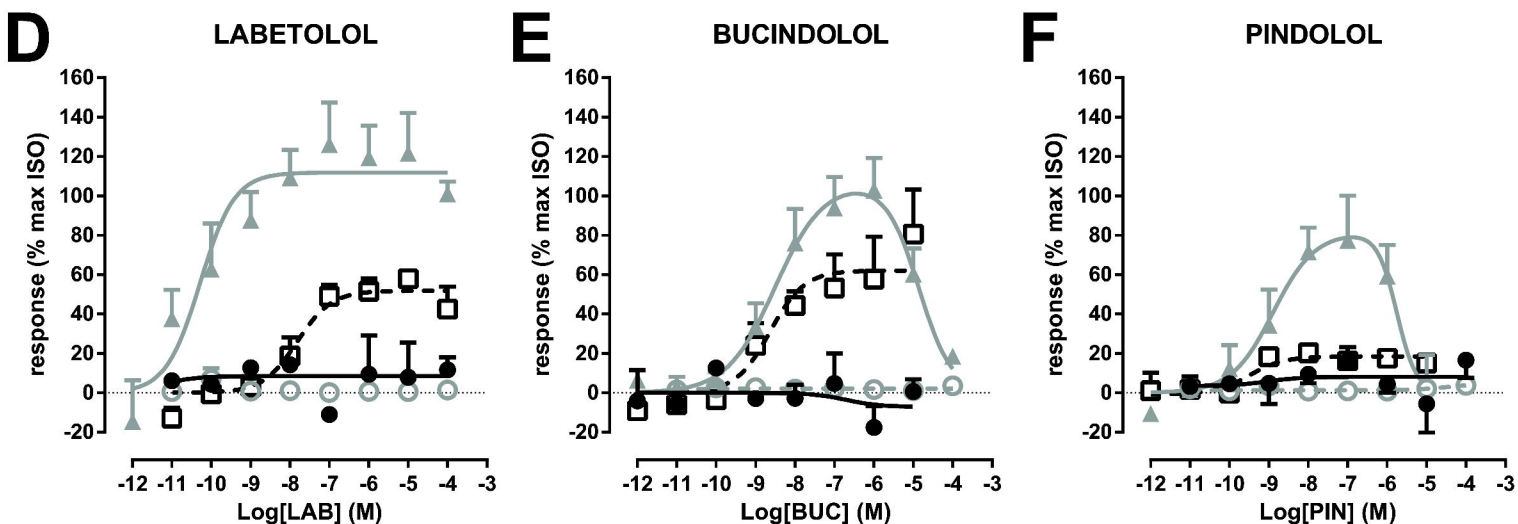
Molecular Pharmacology Fast Forward. Published on December 23, 2013 as DOI: 10.1124/mol.113.088880
This article has not been copyedited and formatted. The final version may differ from this version.



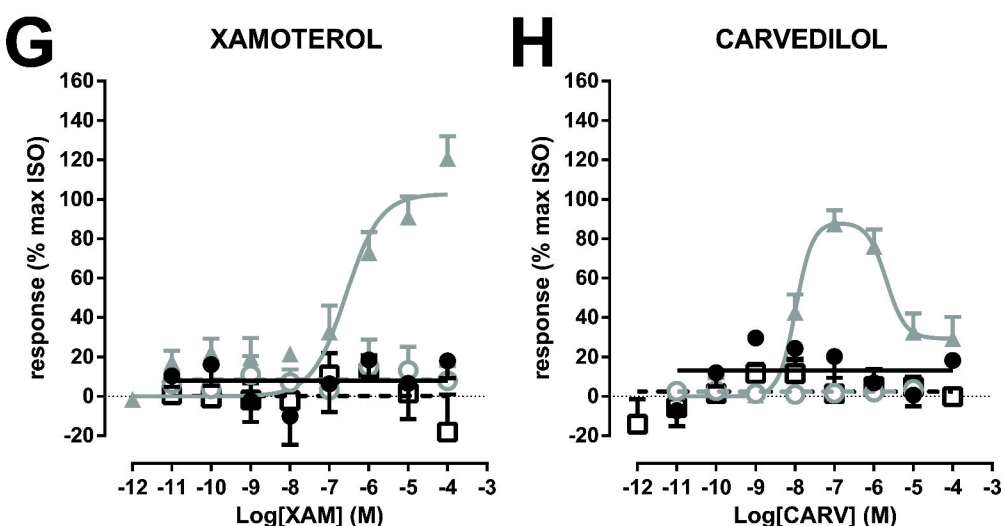
Group II: 3 pathways



Group III: 2 pathways



Group IV: agonist 1 pathway



Group V: inverse agonist 1 pathway

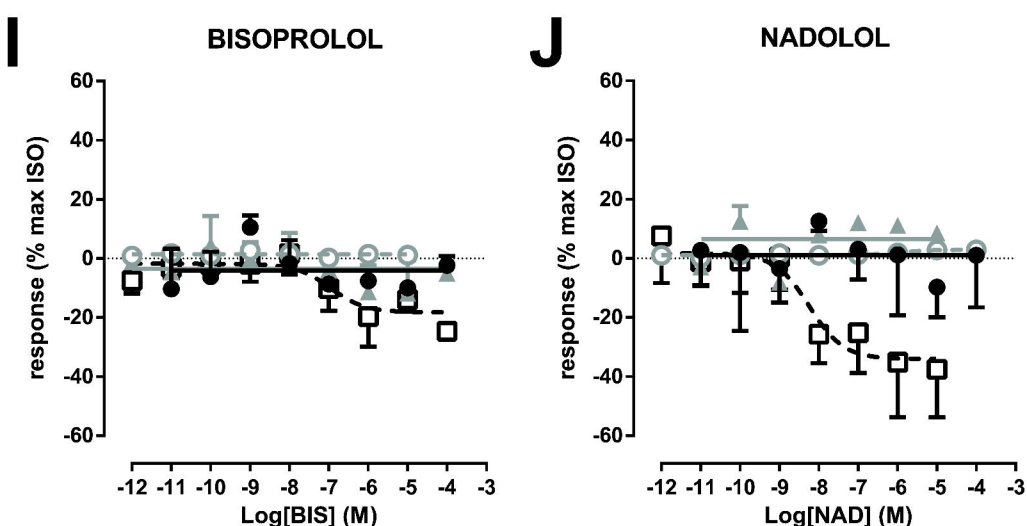


FIGURE 8

